## CHAPTER IV
## RESULTS AND DISCUSSION

In this study, the experiments on the formation of barium sulfate precipitates were systematically carried out in the presence of different three scale inhibitors namely ATMP, DTPMP, and PPCA. For comparison, identical experiments in the absence of scale inhibitors were also performed. The effects of the testing time, the scale inhibitor concentration, and the initial solution pH were investigated. The morphological structure, elemental analysis and particle size distribution of the resulting $BaSO_4$ precipitates were also comparatively studied.
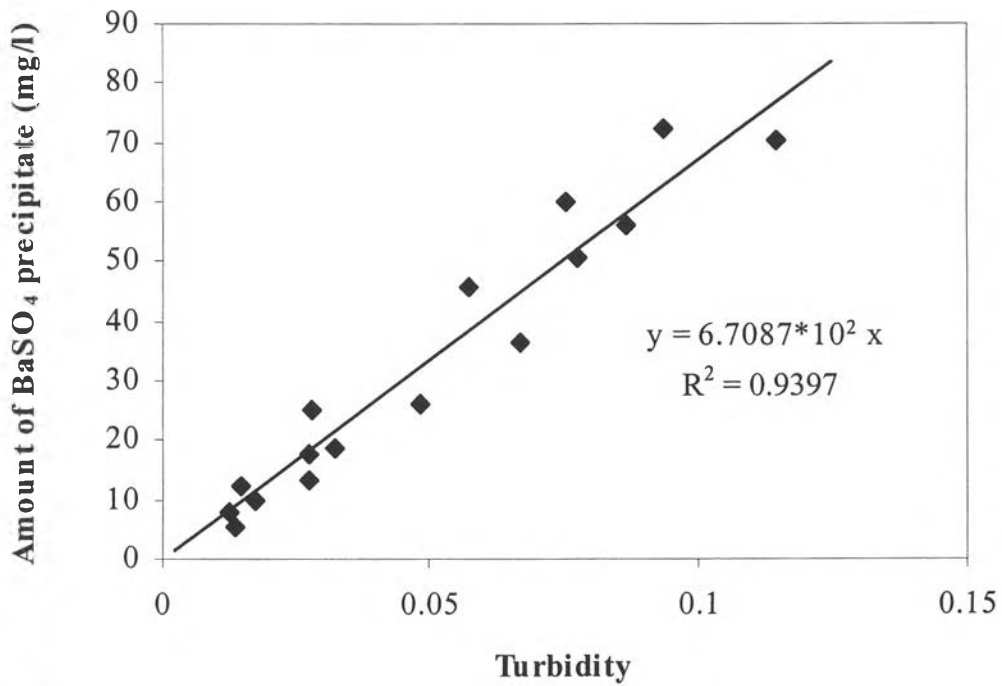
### 4.1 The Correlation between Amount of $BaSO_4$ Precipitates and Turbidities

The correlation between the amount of $BaSO_4$ precipitates and the turbidities measured by a UV-Visible Spectrophotometer at 250 nm is shown in Figure 4.1. It is illustrated that the linear correlation can be suitably represented. The increase in the turbidity was a result of the increase in the amount of $BaSO_4$ precipitates contained in the solution mixtures. In other words, the greater the amount of the $BaSO_4$ precipitates, the larger the extent of UV light absorbed and scattered by such precipitates, resulting in the higher the value of measured turbidity. This correlation could be advantageously used as a calibration curve for converting the turbidity to the amount of the $BaSO_4$ precipitates in next sections.

### 4.2 The Existence of Critical Supersaturation Ratio

The supersaturation ratio (SR) can be expressed as:

$$SR = \frac{a_{Ba^{2+}} \, a_{SO_4^{2-}}}{K_{sp}} \qquad (4.1)$$

**Figure 4.1**  The correlation between the amount of BaSO$_4$ precipitates and the turbidities.

where   $a_{Ba2+}$ denotes activitie of barium ion

   $a_{SO42-}$ denotes activitie of sulfate ion

   $K_{sp}$ is the solubility product of BaSO$_4$ = 1.08 x 10$^{-10}$ M$^2$

The activity is defined as:

$$a_z \quad = \quad f_Z\, C_z \tag{4.2}$$

where   $a_z$  =  activity of z-valent ions (M)

   $C_z$  =  concentration of z-valent ions (M)

   $f_Z$  =  activity coefficient of z-valent ions

Substituting Eq. (4.2) into Eq. (4.1), Eq. (4.1) becomes:

$$SR = \frac{f_{Ba2+} \, f_{SO42-} \, C_{Ba2+} \, C_{SO42-}}{K_{sp}} \qquad (4.3)$$

In order to determine the activity coefficient in dilute solutions, the Debye-Huckel equation (Perrin, 1974) is expressed as follows:

$$\log f_Z = -\frac{A \, Z^2 \, I^{0.5}}{1+I^{0.5}} + 0.1 Z^2 I \qquad (4.4)$$

where   $Z$ = charge of ion

     $I$ = ionic strength (M)

     $A$ = a constant which depends on the temperature

     (at 25°C: A = 0.512)

and the ionic strength is given by the summation as:

$$I = \frac{1}{2} \sum C_z Z^2 \qquad (4.5)$$

Figure 4.2 shows the typically exemplified plot between the amount of the $BaSO_4$ precipitates formed and the supersaturation ratios. The critical supersaturation ratio represents the supersaturation ratio at which the $BaSO_4$ precipitates were significantly observed, resulting from the sudden increase in the turbidity.
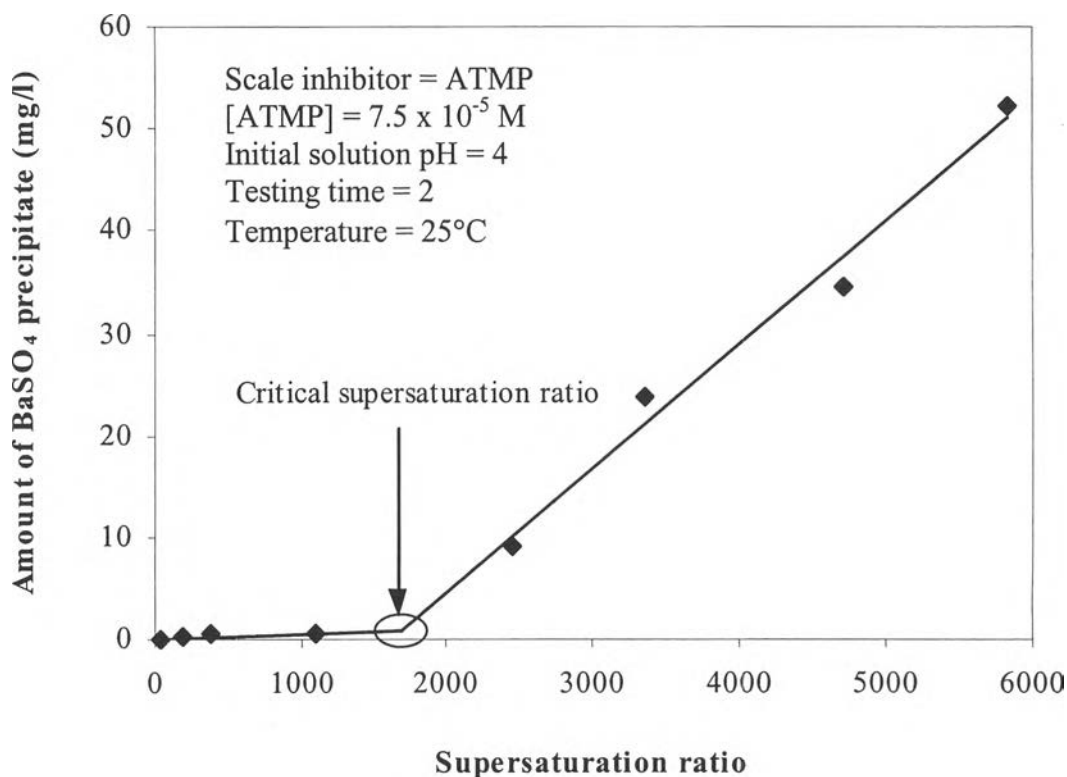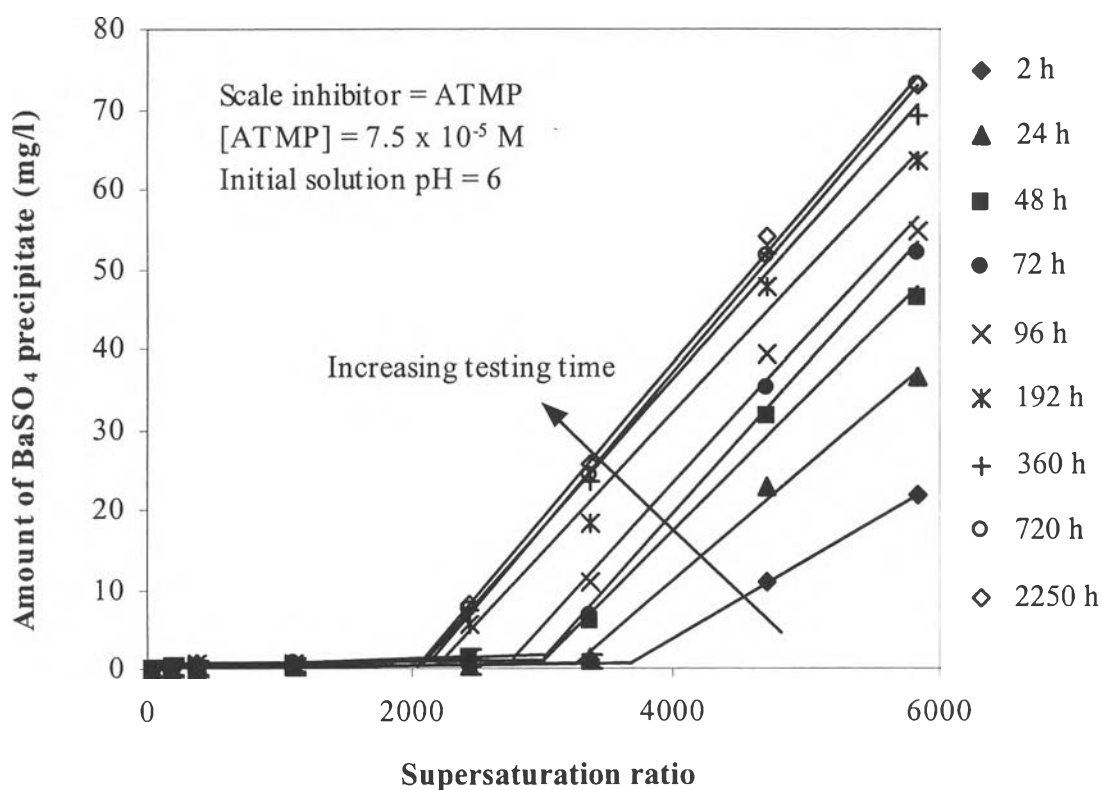
**Figure 4.2** The typical plot between the amount of $BaSO_4$ precipitates and supersaturation ratio to determine the critical supersaturation ratio.

From Figure 4.2, it is apparent that at any given testing time, no $BaSO_4$ precipitate is present in the solution mixtures over the supersaturation ratio range lower than the critical one. According to the fact that $BaSO_4$ is unable to form in a particular period of time, although the supersaturation ratio is slightly greater than the supersaturation ratio at solubility product ($K_{sp}$) of $BaSO_4$, which is equal to 1, it takes the solution mixtures at least a year to form the $BaSO_4$ precipitates (Blaedel and Meloche, 1957). It is not possible to perform the experiments at the SR value close to unity. Hence, in this work, the critical supersaturation ratios at different testing times were then used as an index to evaluate the effect of the scale inhibitors on the $BaSO_4$ scale precipitation.
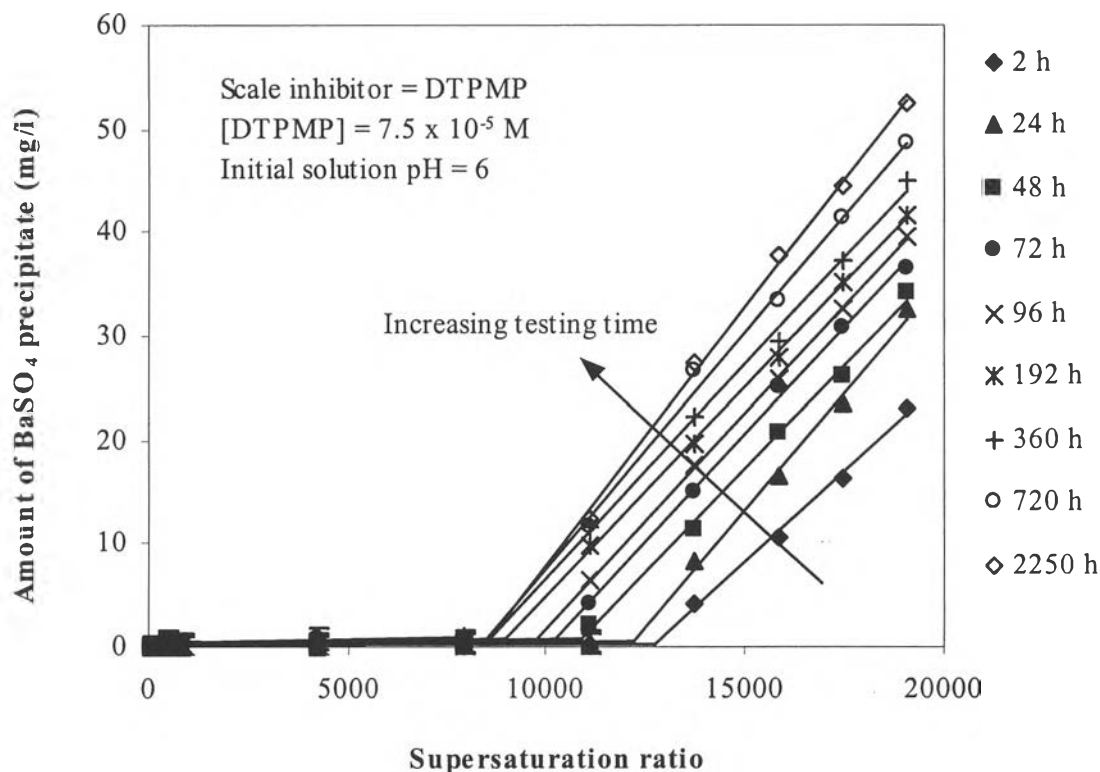
### 4.3    The Effect of Testing Time

4.3.1    The Effect of Testing Time on the Critical Supersaturation Ratio
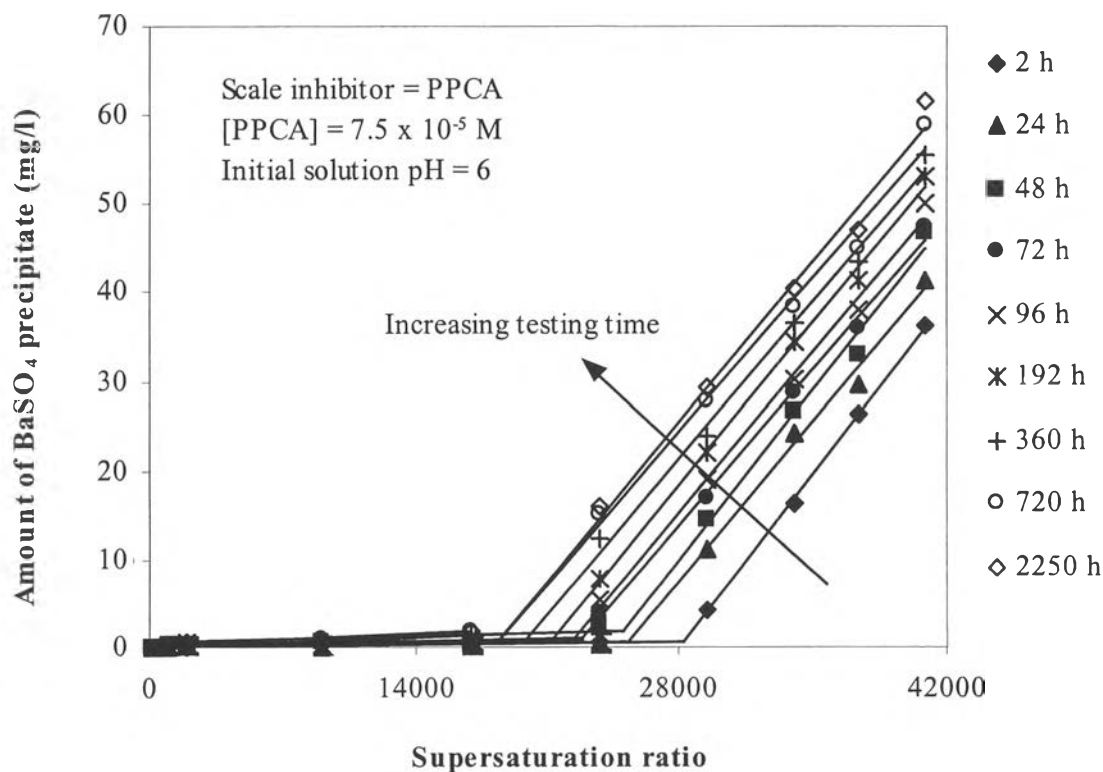
The effect of testing time for $BaSO_4$ precipitation for three scale inhibitors is shown in Figures 4.3 – 4.5.  The testing times in this study were in the range of 2 – 2,250 h.  It was shown that an increase in the testing time resulted in decreasing the critical supersaturation ratio.  However, the critical supersaturation ratio was eventually no longer decreased at virtually long testing time.  The example of the typically replotted correlation between the testing time and the critical supersaturation ratio obtained from Figure 4.3 is consequently shown in Figure 4.6.  The constant value of the critical supersaturation ratio is the maximum level for preventing $BaSO_4$ scale precipitation at given conditions because $BaSO_4$ scale will precipitate out if supersaturation ratio is greater than this constant value.



**Figure 4.3**    The typical plots between the amount of $BaSO_4$ precipitates and supersaturation ratio for different testing times in the presence of ATMP.

**Figure 4.4** The typical plots between the amount of $BaSO_4$ precipitates and supersaturation ratio for different testing times in the presence of DTPMP.



**Figure 4.5** The typical plots between the amount of $BaSO_4$ precipitates and supersaturation ratio for different testing times in the presence of PPCA.
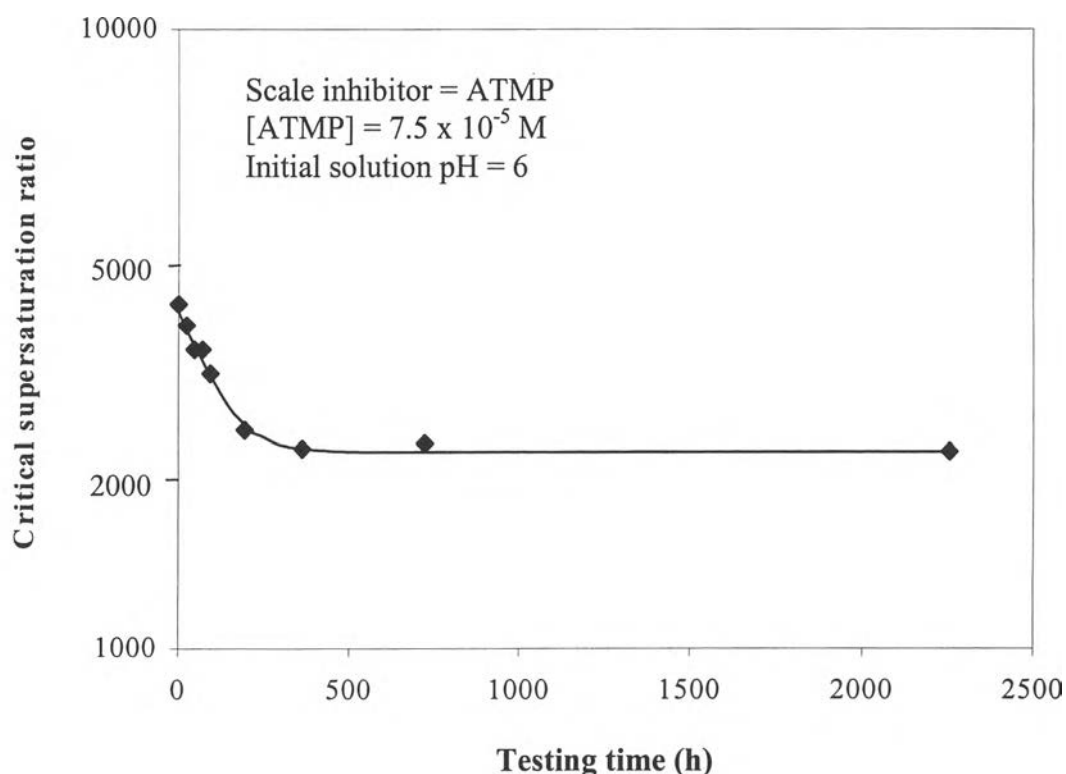
**Figure 4.6** The critical supersaturation ratio with different testing times.

4.3.2    The Effect of Testing Time on the Particle Size Distribution and the Mean Diameter of BaSO$_4$ Precipitates

The particle size distribution of the BaSO$_4$ precipitates forming in different testing times for three scale inhibitors is shown in Figures 4.7 – 4.9. The results illustrate that for any scale inhibitor, the broader particle size distribution was observed with increasing the testing time. It can be explained that for a given precipitating condition, the BaSO$_4$ particles of few specific sizes preferentially form at the first period of the testing time and become larger in size when the testing time increases. For other sizes of the BaSO$_4$ particles, they require the longer testing time to nucleate and then grow after some portions of scale inhibitors are utilized, leaving less amount of scale inhibitor molecules for BaSO$_4$ scale inhibition. Therefore, the mean diameter of the BaSO$_4$ particles obtained from the particle size distribution significantly increased with increasing the testing time until 48 h. However, the mean diameter eventually becomes consistent beyond the testing time of 48 h as shown in Figures 4.10 – 4.12. In addition, the effect of types of scale inhibitors will be discussed later.
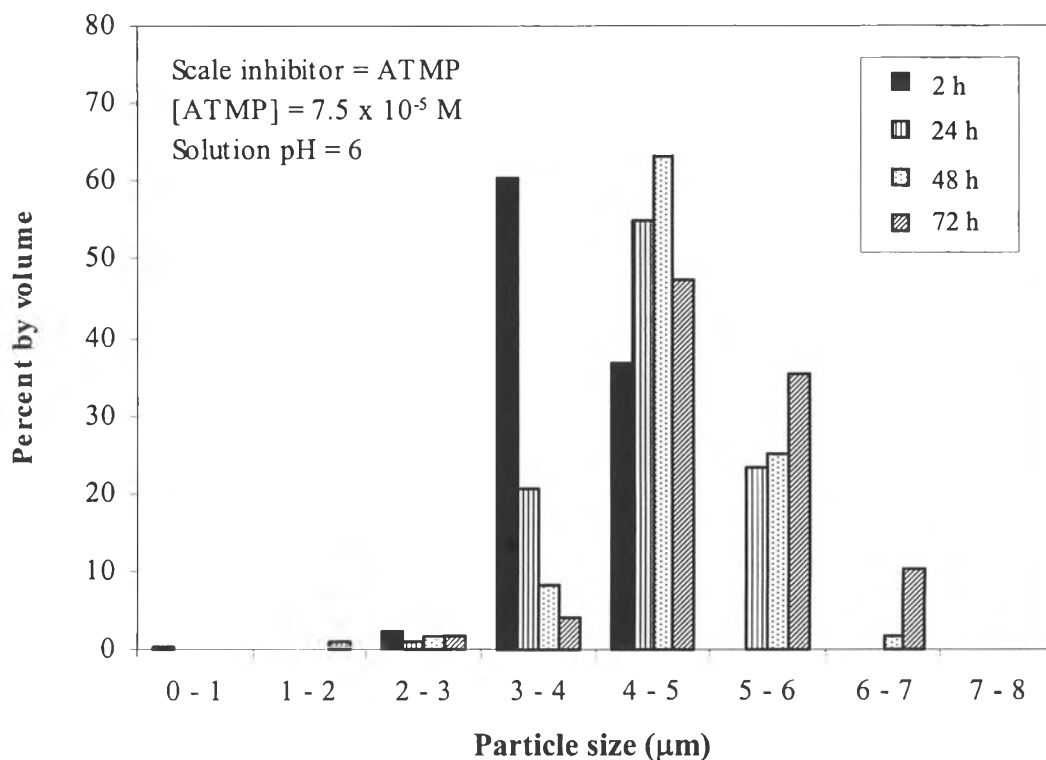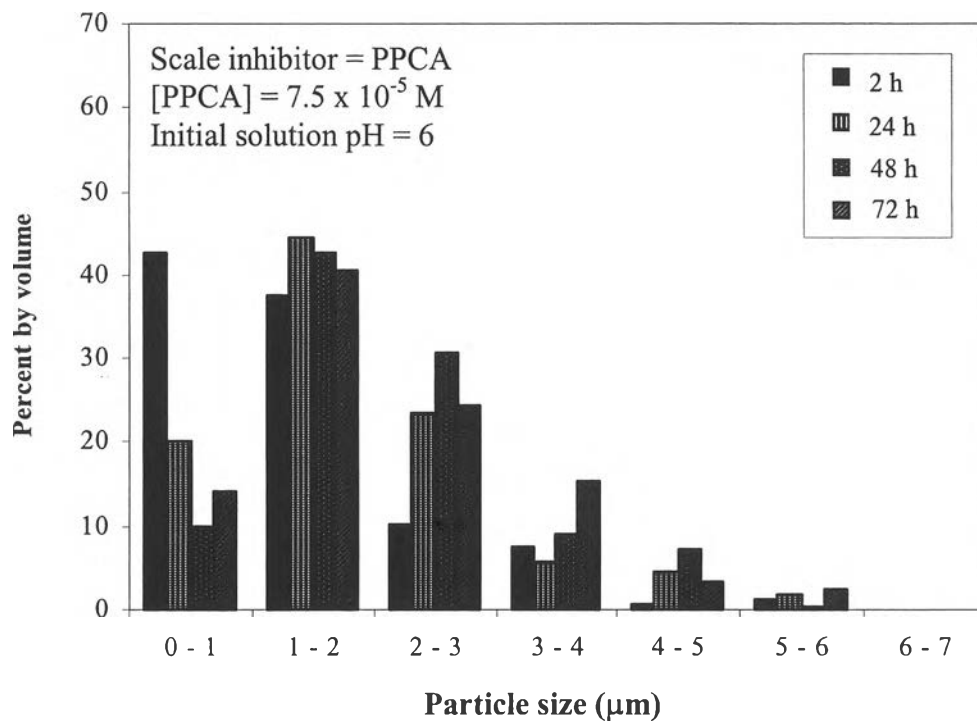
**Figure 4.7** The effect of testing time on the particle size distribution of the BaSO$_4$ precipitates in the presence of ATMP.
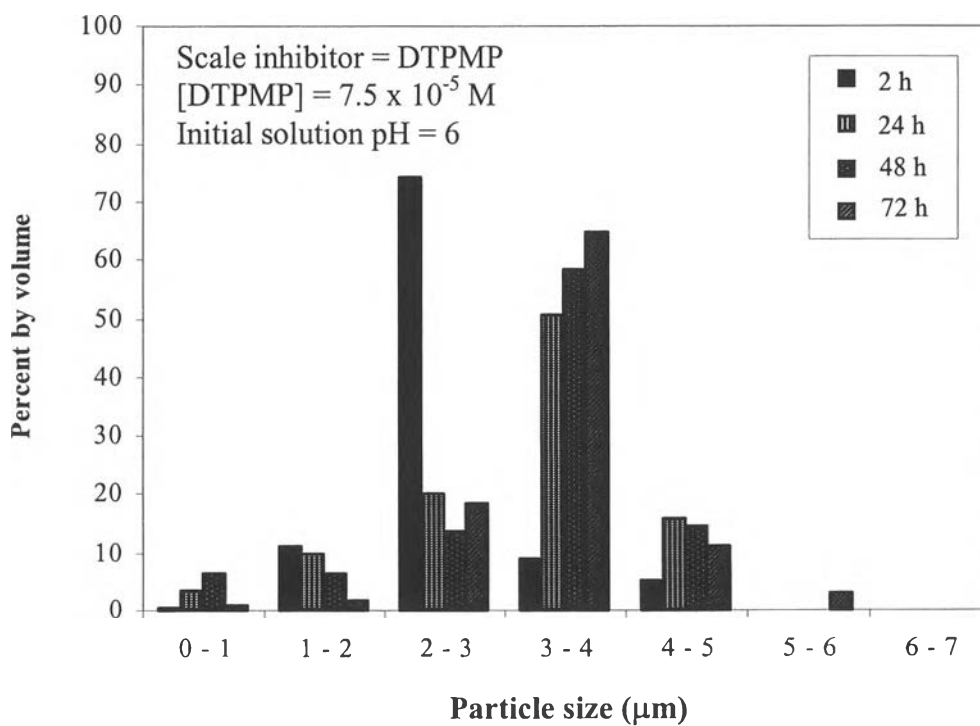


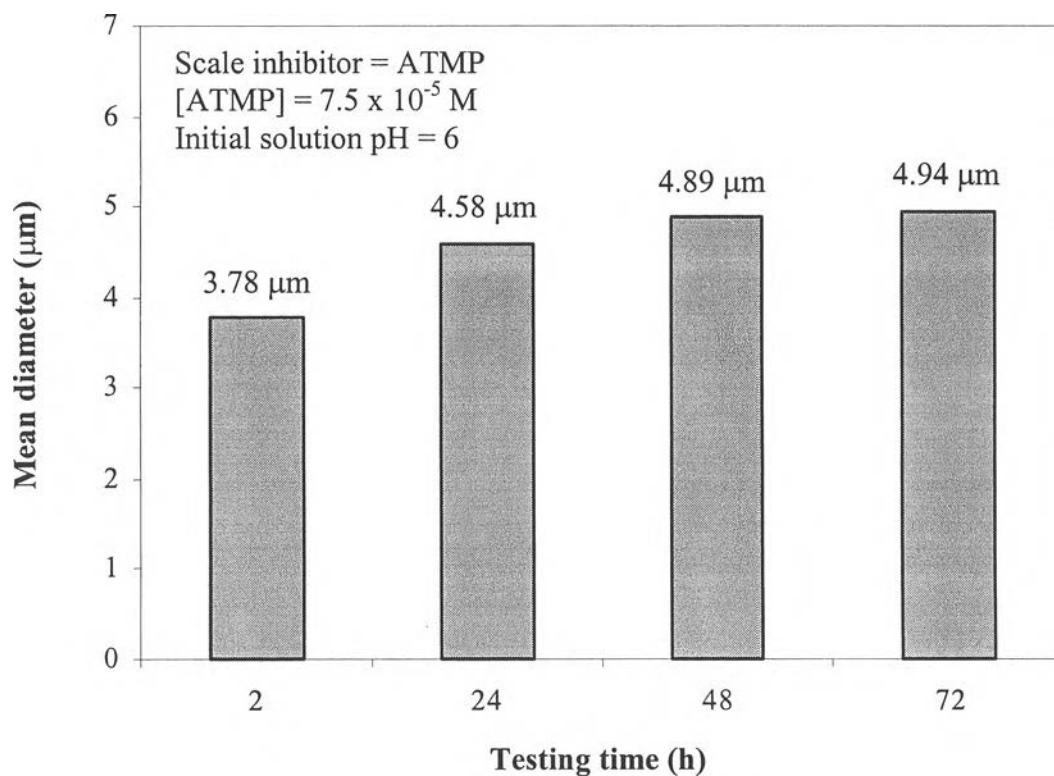**Figure 4.8** The effect of testing time on the particle size distribution of the BaSO$_4$ precipitates in the presence of DTPMP.
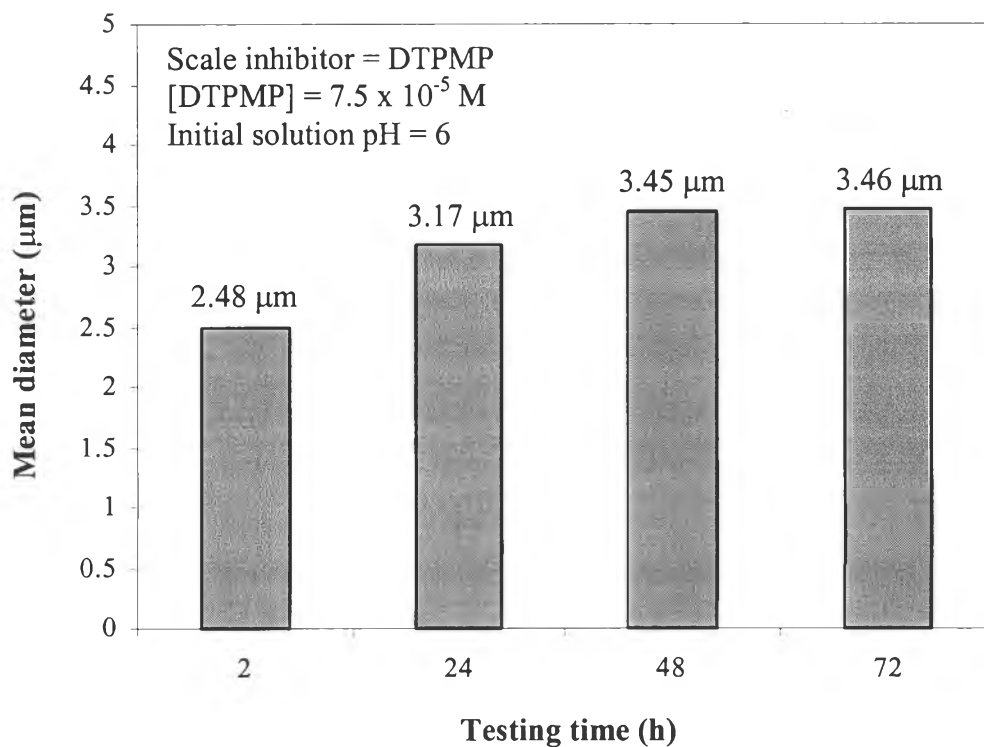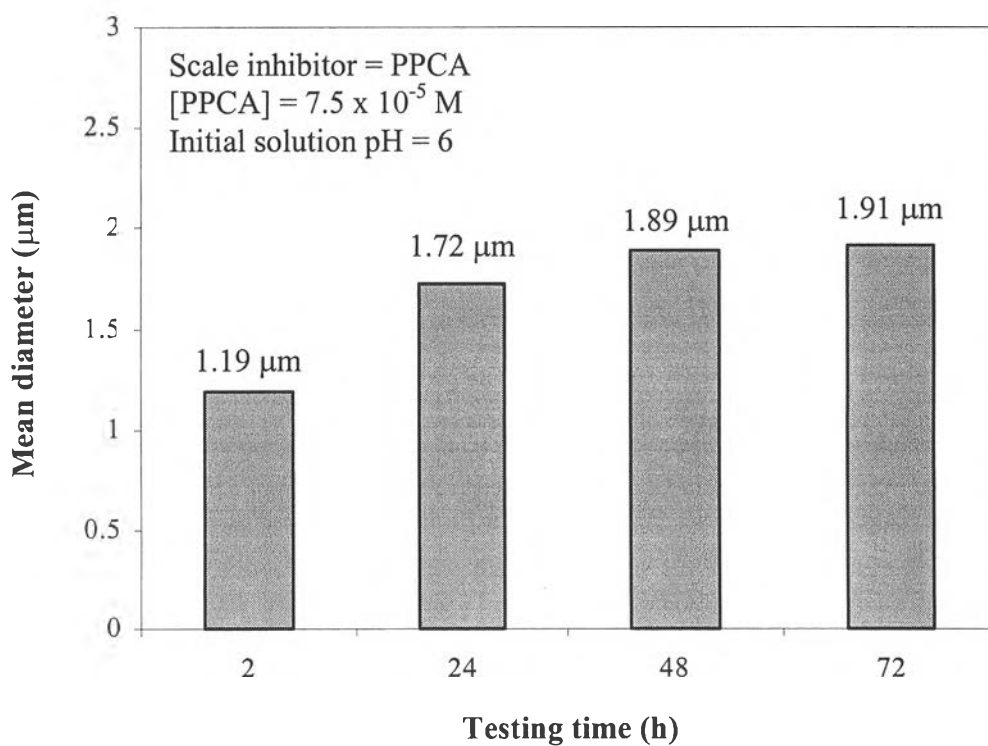
**Figure 4.9** The effect of testing time on the particle size distribution of the BaSO$_4$ precipitates in the presence of PPCA.



**Figure 4.10** The effect of testing time on the mean diameter of the BaSO$_4$ precipitates in the presence of ATMP.

**Figure 4.11** The effect of testing time on the mean diameter of the BaSO$_4$ precipitates in the presence of DTPMP.



**Figure 4.12** The effect of testing time on the mean diameter of the BaSO$_4$ precipitates in the presence of PPCA.

## 4.4 The Effect of Scale Inhibitor Concentration
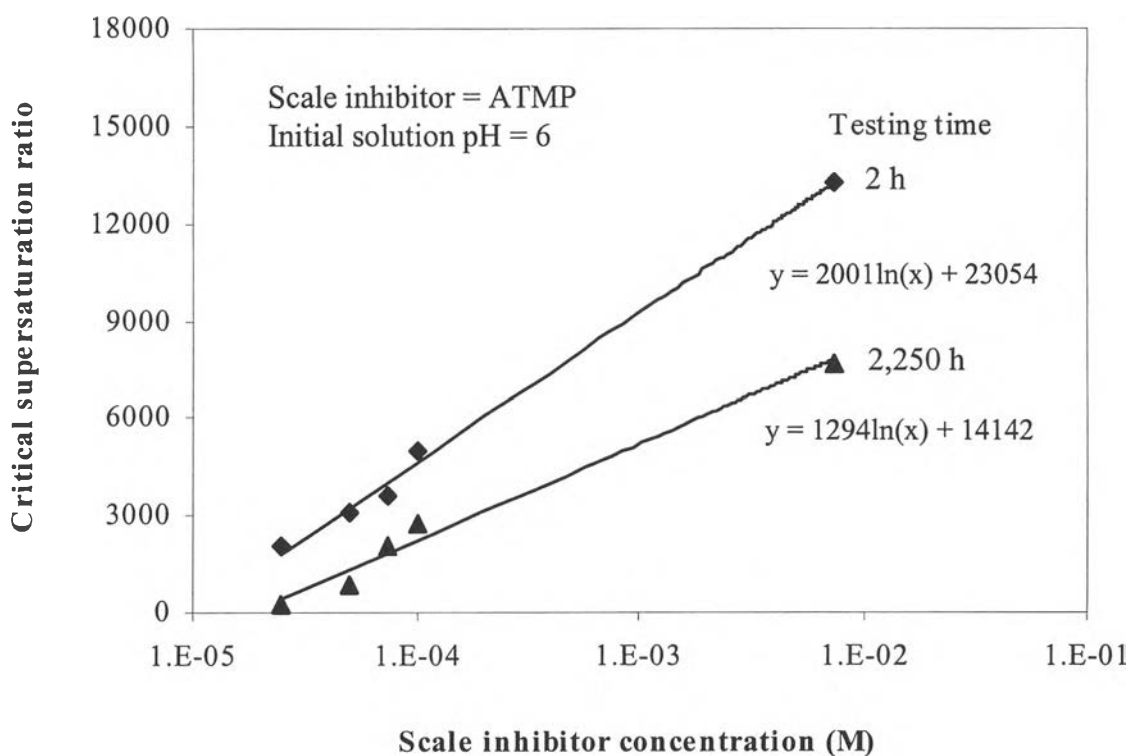
4.4.1 <u>The Effect of Scale Inhibitor Concentration on the Critical Supersaturation Ratio</u>

The effect of scale inhibitor concentration on the critical supersaturation ratios was studied at initial solution pH of 6 both in the presence and in the absence of ATMP, DTPMP, and PPCA. The concentrations of these scale inhibitors were in the range of $2.5 \times 10^{-5} - 7.5 \times 10^{-3}$ M. Normally, low concentrations of scale inhibitors ranging from $2.5 \times 10^{-5}$ to $1.0 \times 10^{-4}$ M are used in the actual oil fields and known as the threshold concentration (Sorbie *et al.*, 1994 and Putnis *et al.*, 1995). On the contrary, the very high concentration of scale inhibitors such as $7.5 \times 10^{-3}$ M may occasionally be used in some oil fields which have extremely serious scaling problems. Figure 4.13 shows the variation of critical supersaturation ratios with the testing times over two concentrations of ATMP as compared to the condition without ATMP. It is shown that the scale inhibitor can delay the formation of $BaSO_4$ precipitates because the critical supersaturation ratios observed in the presence of the scale inhibitors are much higher than that in the absence of the inhibitor at the same testing time. From Figure 4.13, the results show that for any given ATMP concentration, the supersaturation ratios decrease with increasing the testing time and tend to be constant at very long testing times. In the presence of ATMP, it is obvious that at lower concentrations, the critical supersaturation ratio decreased faster with increasing the testing time than at higher concentrations. It can be explained that at lower scale inhibitor concentrations, less number of active scale inhibitor molecules is available for adsorbing and then blocking the forming $BaSO_4$ precipitates. Therefore, when the testing time is increased, the $BaSO_4$ precipitates can form and grow easier. In contrast, at higher scale inhibitor concentrations, the number of active molecules is greater, resulting in the more consistency of the critical supersaturation ratios with the testing times. However, in the absence of scale inhibitors, the gradual decrease in the critical supersaturation ratios with increasing the testing times was observed. In addition, the critical supersaturation ratio tends to continuously and gradually decrease until reaching the solubility product ($K_{sp}$) at extremely long testing time.
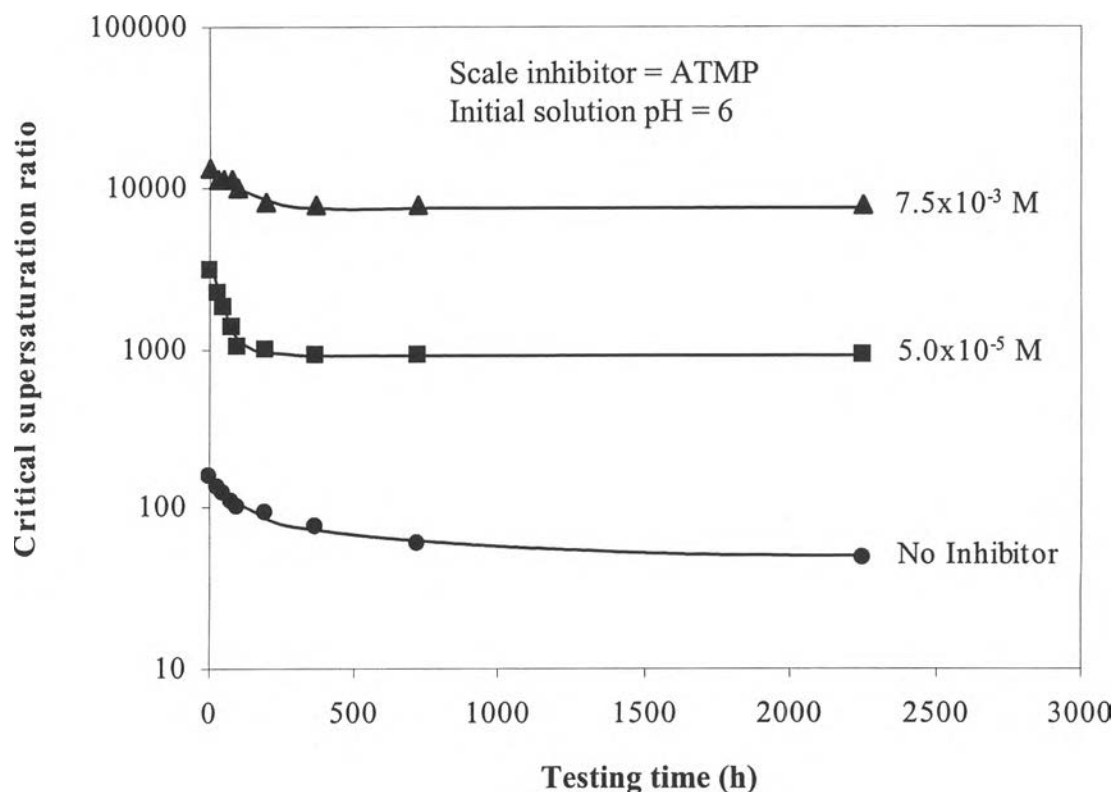
**Figure 4.13** The variation of the critical supersaturation ratios with the testing times for different scale inhibitor (ATMP) concentrations.

Moreover, from Figure 4.13 the correlation between the scale inhibitor concentration and the critical supersaturation ratio in the presence of ATMP can be consequently plotted in Figure 4.14. In the presence of DTPMP and PPCA, the correlations are shown in Figures 4.15 and 4.16, respectively. It is obviously seen that at exemplified testing times of either 2 or 2,250 h for all three scale inhibitors, the critical supersaturation ratio is represented as a linear function of the logarithm of the scale inhibitor concentration. This correlation could be usefully applied for the oil fields. At any given testing time, the area under each curve represents the no-precipitation zone whereas the area above each curve represents the precipitation zone. Therefore, the appropriate concentration of the scale inhibitors can be selected to use in the oil fields whose particular supersaturation ratio is known and a desirable squeeze lifetime is required.

**Figure 4.14** The effect of scale inhibitor (ATMP) concentration on the critical supersaturation ratio.
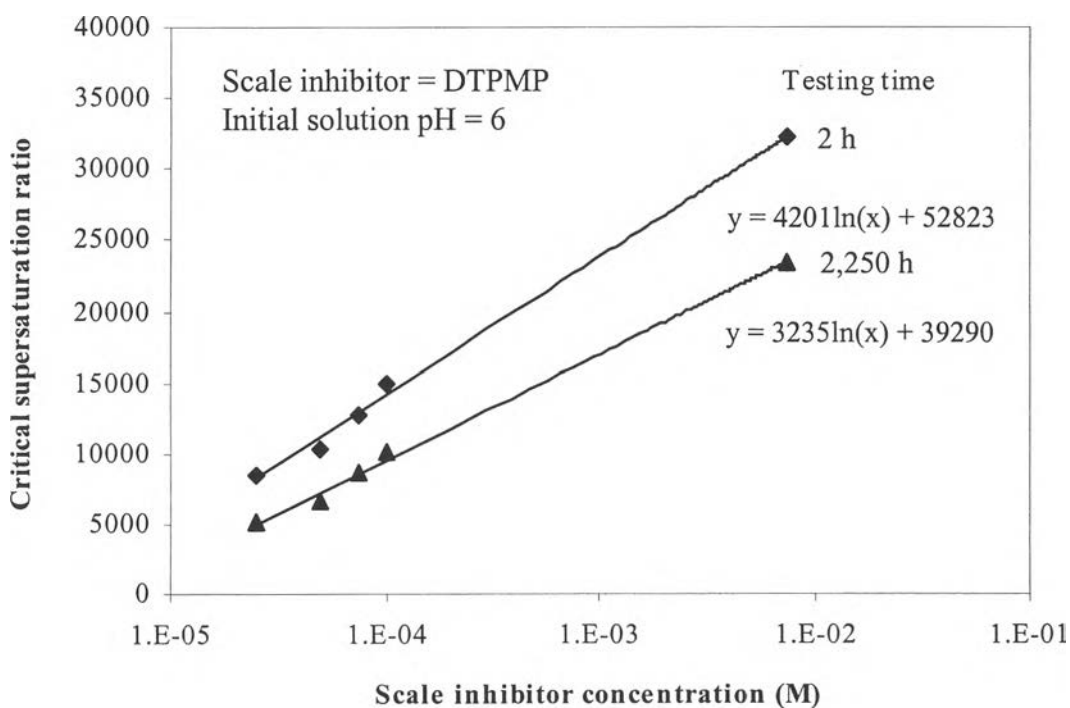


**Figure 4.15** The effect of scale inhibitor (DTPMP) concentration on the critical supersaturation ratio.

T 206.93 667
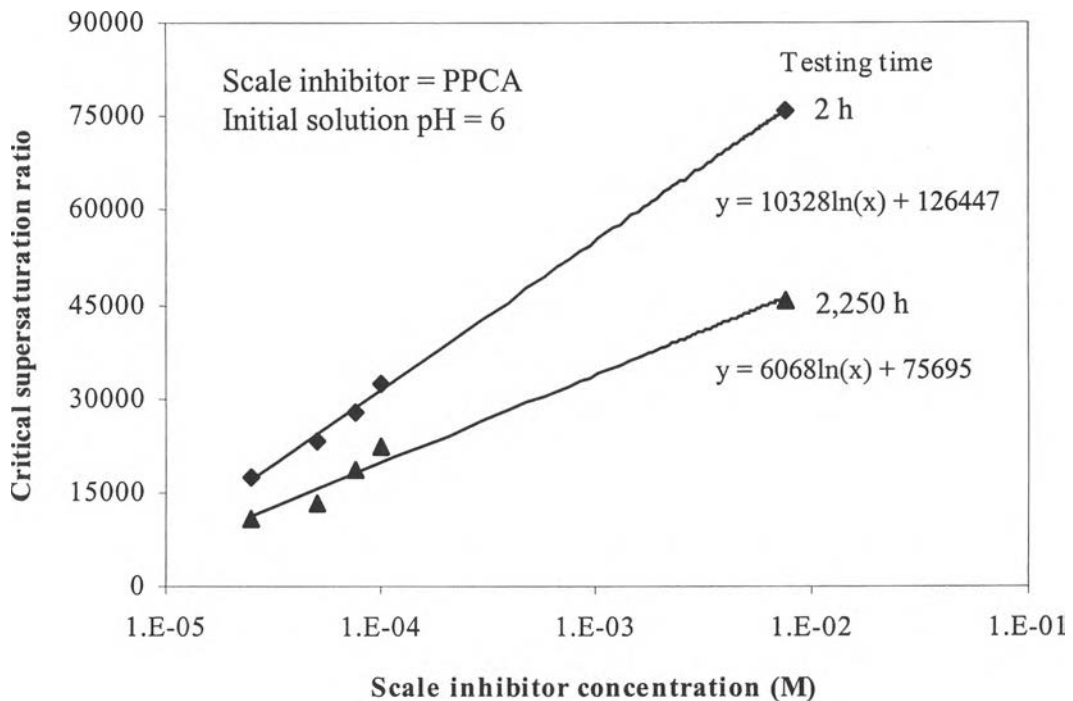
**Figure 4.16** The effect of scale inhibitor (PPCA) concentration on the critical supersaturation ratio.

### 4.4.2 The Effect of Scale Inhibitor Concentration on the Morphology of BaSO₄ Precipitates

The morphologies of the $BaSO_4$ precipitates formed at various scale inhibitor concentrations are shown in Figure 4.17. It can be seen that the concentration of scale inhibitors plays an important role on the morphological structure and the particle size of the $BaSO_4$ precipitates. The higher the concentration of the scale inhibitors was used, the smaller and more spherical the particle of $BaSO_4$ precipitates was observed, resulting from the higher scale inhibitor molecules available for adsorbing and blocking on more active growth sites around the forming $BaSO_4$ precipitates.
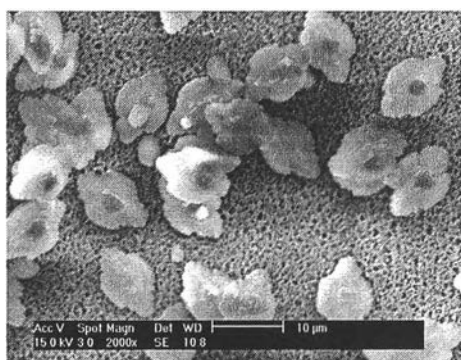
(a) [Inhibitor] = 0 M (2000X)
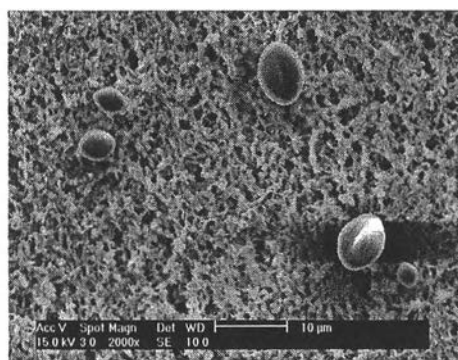
(b) [Inhibitor] = 2.5 x 10$^{-5}$ M (2000X)
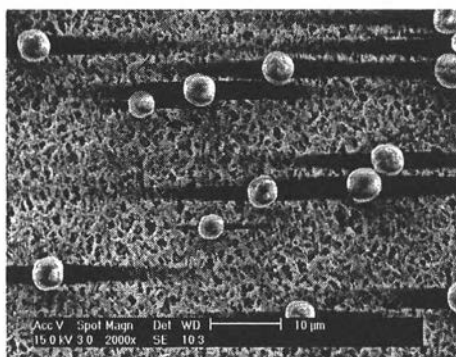
(c) [Inhibitor] = 7.5 x 10$^{-5}$ M (2000X)

**Figure 4.17** The morphological structures of the BaSO$_4$ precipitates for different scale inhibitor concentrations: (a) in the absence of scale inhibitor (ATMP), SR = 380; (b) and (c) in the presence of ATMP, SR = 6,515 and 5,832, respectively; testing time = 2 h.

### 4.4.3 The Effect of Scale Inhibitor Concentration on the Particle Size Distribution and the Mean Diameter of BaSO$_4$ Precipitates

Figures 4.18 – 4.23 display the effect of scale inhibitor concentration on the particle size distribution and the mean diameter of the BaSO$_4$ precipitates, respectively for all three scale inhibitors. The results reveal that the higher the scale inhibitor concentration was used, the broader the particle size distribution and the smaller the mean diameter of the BaSO$_4$ particles were apparently observed. The explanation is that the higher number of the scale inhibitor molecules provides the higher capability of adsorbing onto the forming BaSO$_4$ precipitate, resulting in the blockage of that nucleated scale. New nucleated BaSO$_4$ particles are repeatedly nucleated, further grown, and finally blocked. Consequently, the broader particle size distribution and smaller mean diameter of BaSO$_4$ particles are attained.
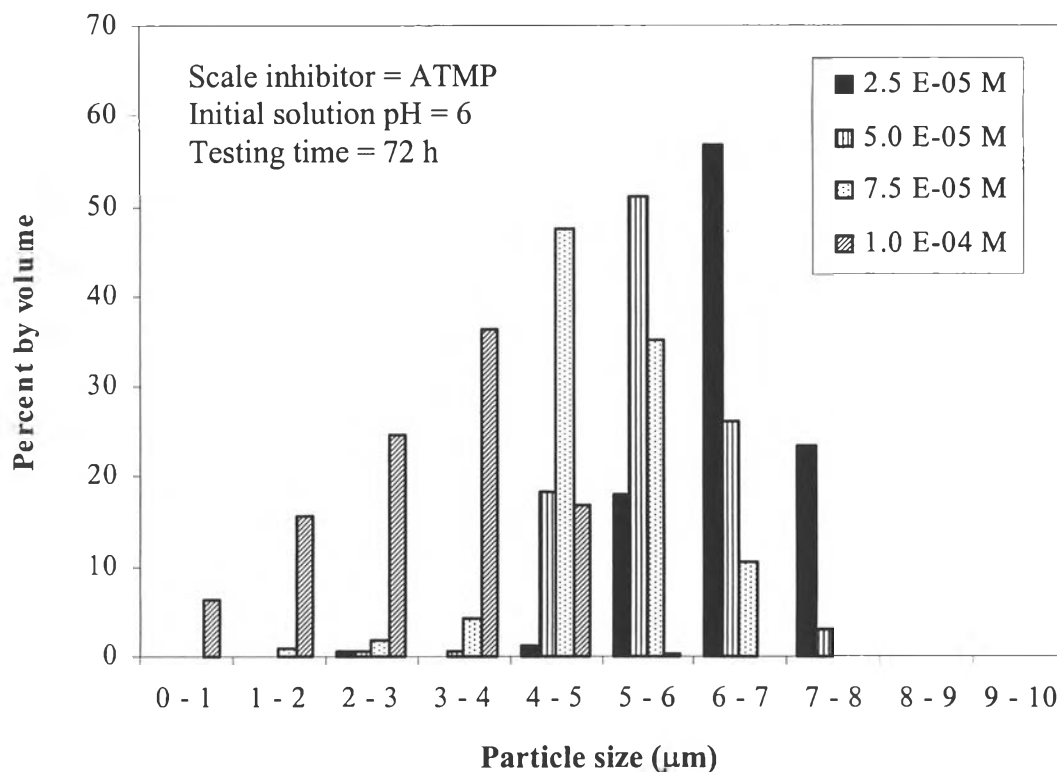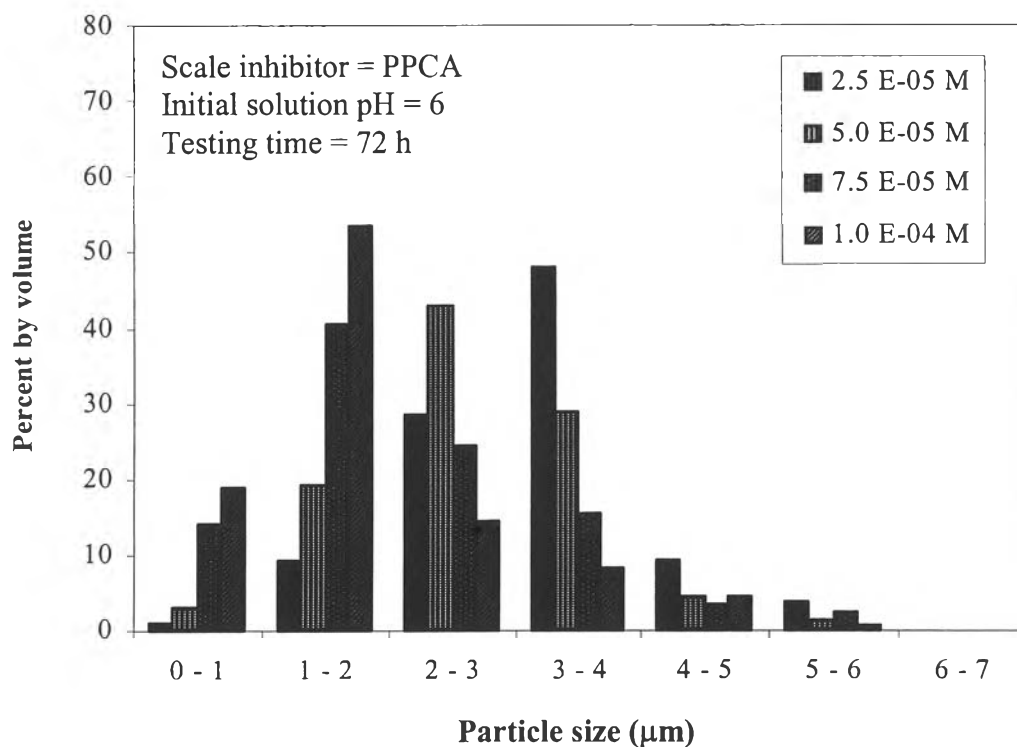
**Figure 4.18** The effect of scale inhibitor (ATMP) concentration on the particle size distribution of the BaSO$_4$ precipitates.
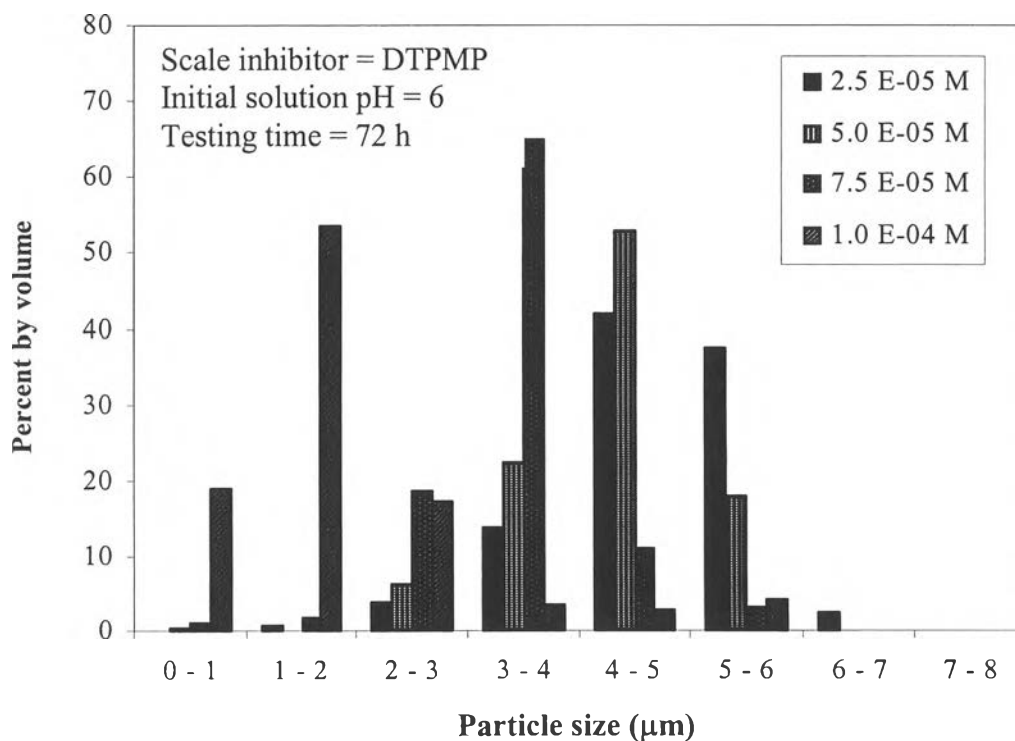

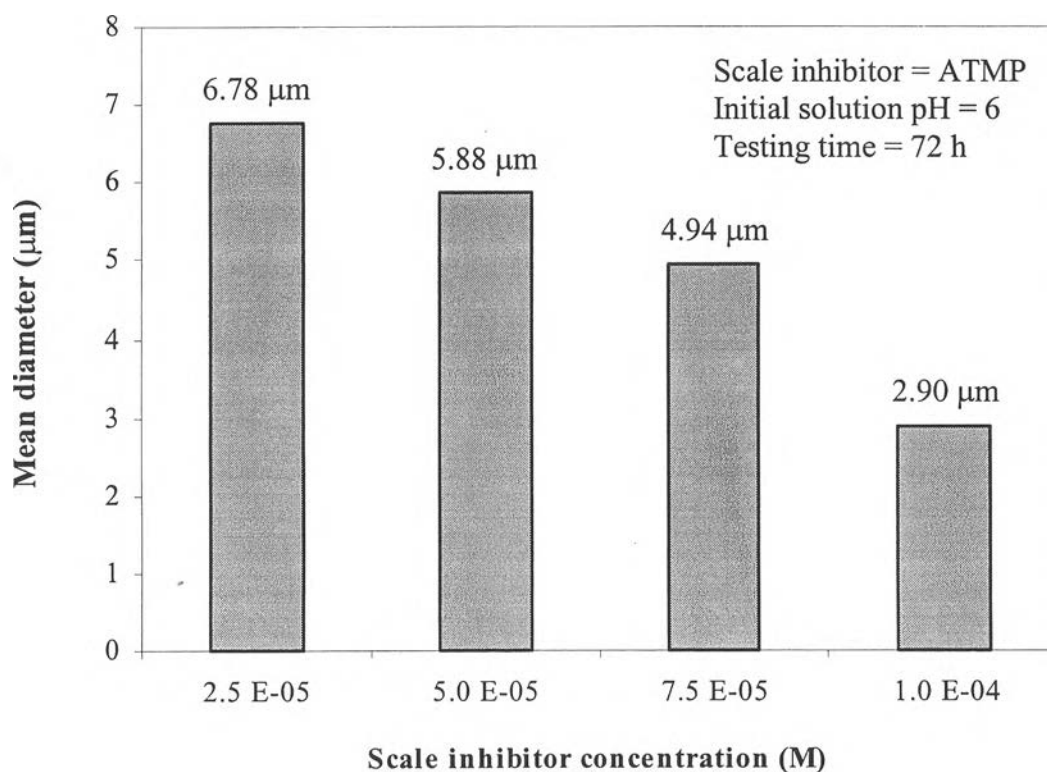
**Figure 4.19** The effect of scale inhibitor (DTPMP) concentration on the particle size distribution of the BaSO$_4$ precipitates.
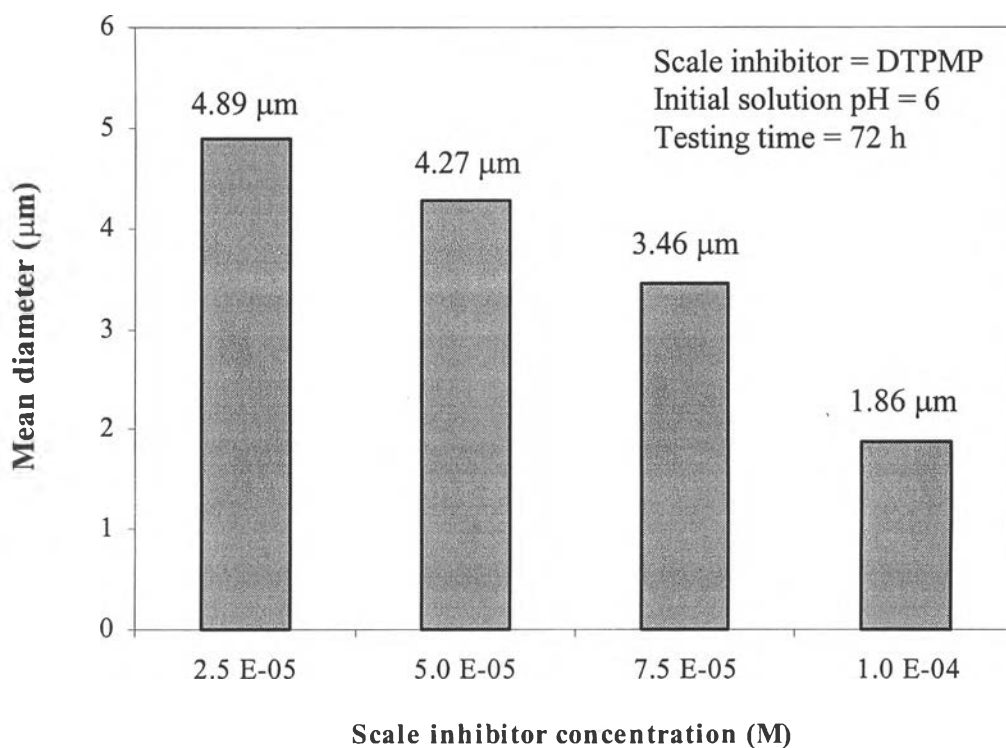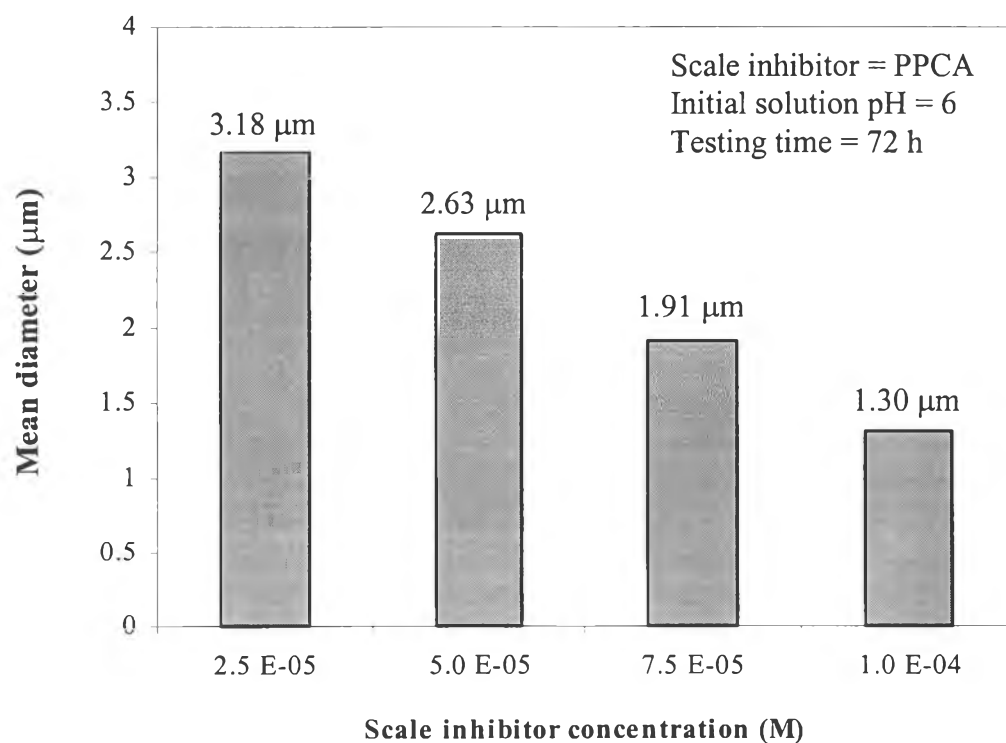
**Figure 4.20** The effect of scale inhibitor (PPCA) concentration on the particle size distribution of the BaSO$_4$ precipitates.



**Figure 4.21** The effect of scale inhibitor (ATMP) concentration on the mean diameter of the BaSO$_4$ precipitates.

**Figure 4.22** The effect of scale inhibitor (DTPMP) concentration on the mean diameter of the $BaSO_4$ precipitates.



**Figure 4.23** The effect of scale inhibitor (PPCA) concentration on the mean diameter of the $BaSO_4$ precipitates.
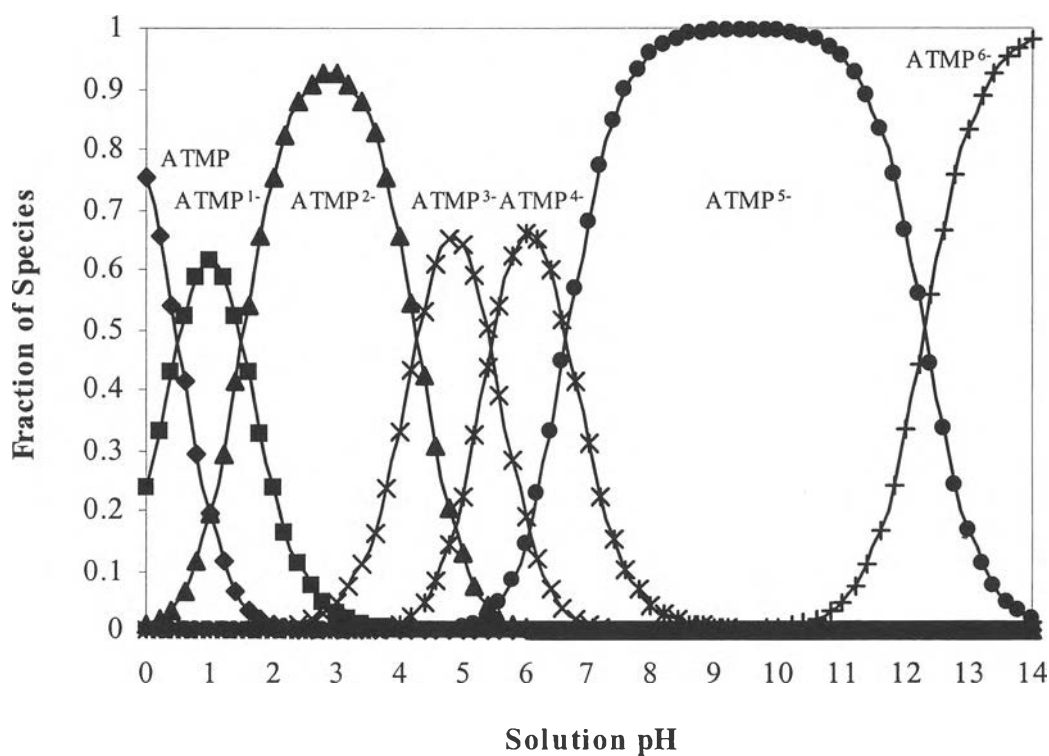
## 4.5  The Effect of Initial Solution pH

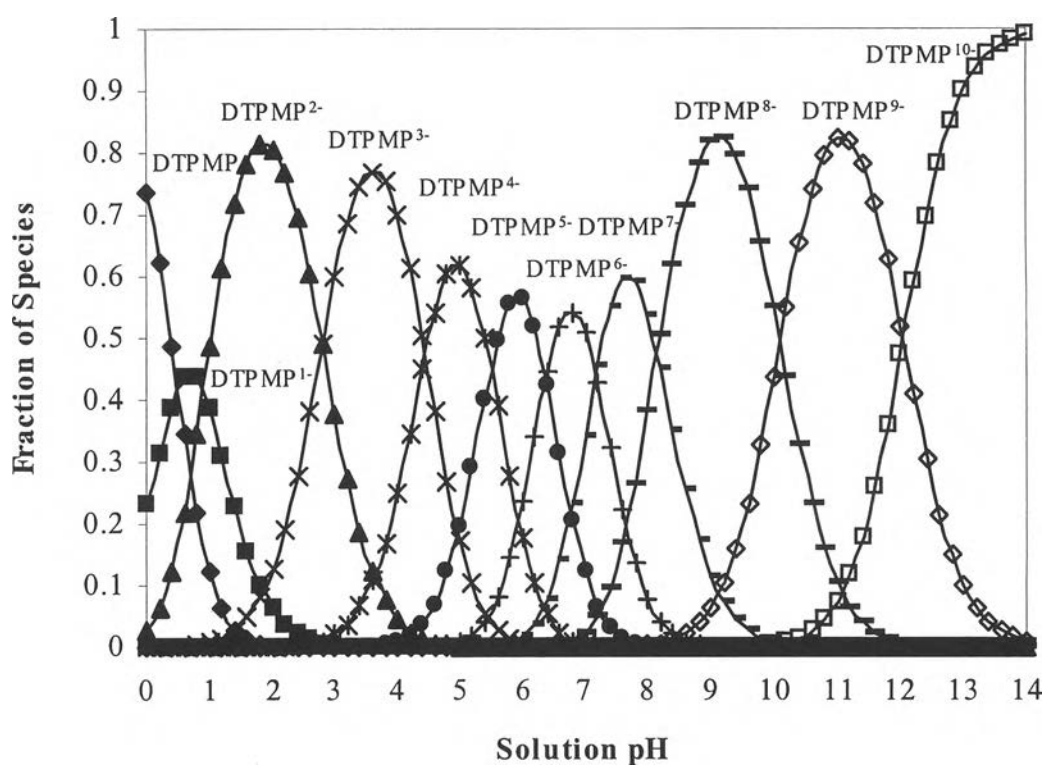### 4.5.1  The Effect of Initial Solution pH on the Critical Supersaturation Ratio

The effect of initial solution pH on the critical supersaturation ratio was studied at scale inhibitor concentration of 7.5 x $10^{-5}$ M in the presence of ATMP, DTPMP, and PPCA.  The initial solution pHs studied were 4, 6, and 8 where the pH range of 4 – 7 or higher are usually found in the real conditions (Yuan $et$ $al.$, 1993). Figure 4.24 illustrates the critical supersaturation ratio as a function of testing time over the range of pH studied.  It is obvious that the critical supersaturation ratio at pH 4 drastically decrease with increasing the testing time when the testing time was below 96 h.  In contrast, at both pH 6 and 8, the critical supersaturation ratio insignificantly decreased in the first period of testing times until 192 h and then became consistent beyond 192 h.  The results demonstrate that at pH 4, the scale inhibitor molecules are less deprotonated than at pH 6 and 8, respectively, as seen from the deprotonation curves of ATMP and DTPMP in Figures 4.25 and 4.26.  Therefore, the capability of adsorbing and blocking the growth of the forming $BaSO_4$ precipitates at pH 4 is less effective than at higher pHs (He $et$ $al.$, 1996).  Subsequently, the data in the presence of ATMP obtained from Figure 4.24 were then replotted as the correlation between the initial solution pH and the critical supersaturation ratio as shown in Figure 4.27.  In the same manner, Figures 4.28 and 4.29 show the correlations in cases of DTPMP and PPCA, respectively.  It is clearly seen that at exemplified testing times of either 2 or 2,250 h for any scale inhibitor, the critical supersaturation ratio varies linearly with the initial solution pH.  This correlation could be practically applied for the actual oil production system.  At any given testing times, the area under and above each curve represented the no-precipitation and precipitation zones, respectively as described earlier.  Hence, the suitable initial solution pH could be chosen to apply for the oil fields whose particular supersaturation ratio is existed at any values to exclude the $BaSO_4$ scaling problem from actual oilfields.
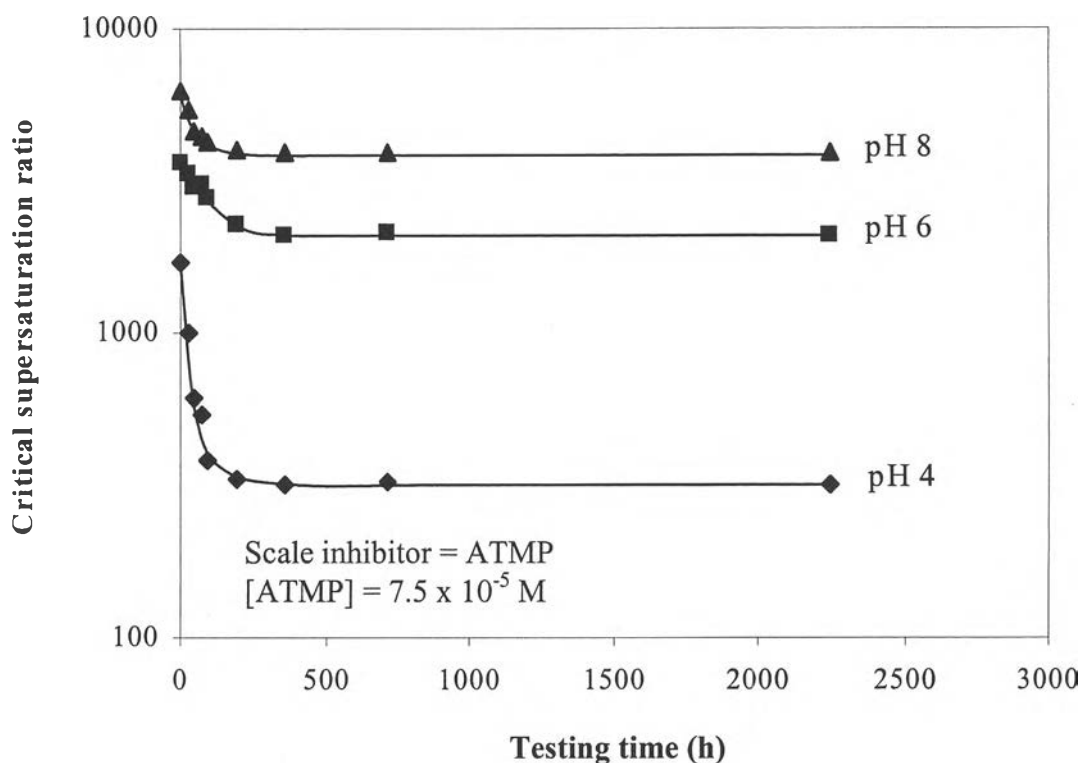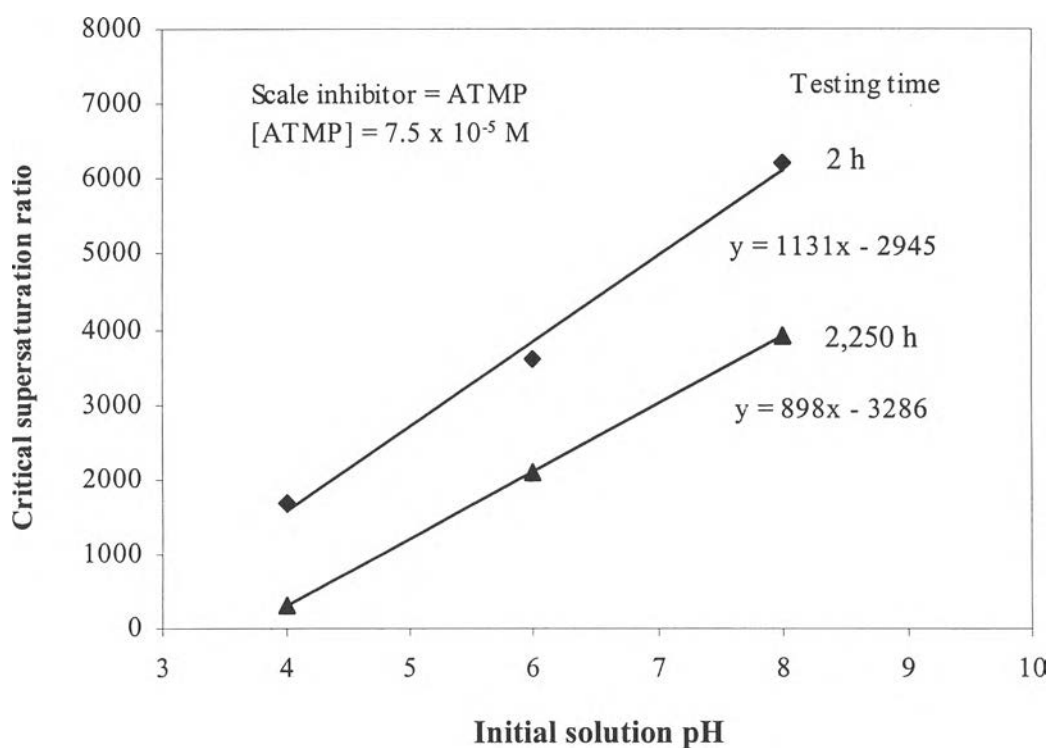
**Figure 4.24** The variation of the critical supersaturation ratios with the testing times for different initial solution pHs.
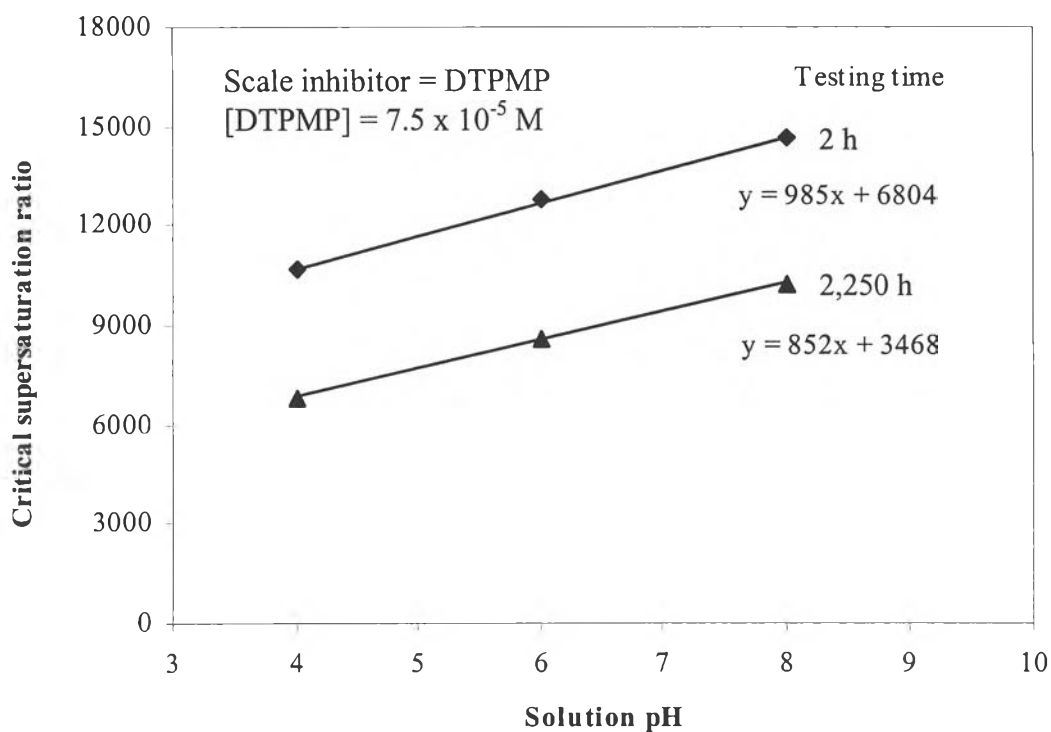


**Figure 4.25** The deprotonation curve of ATMP and the resulting species composition as a function of solution pH.
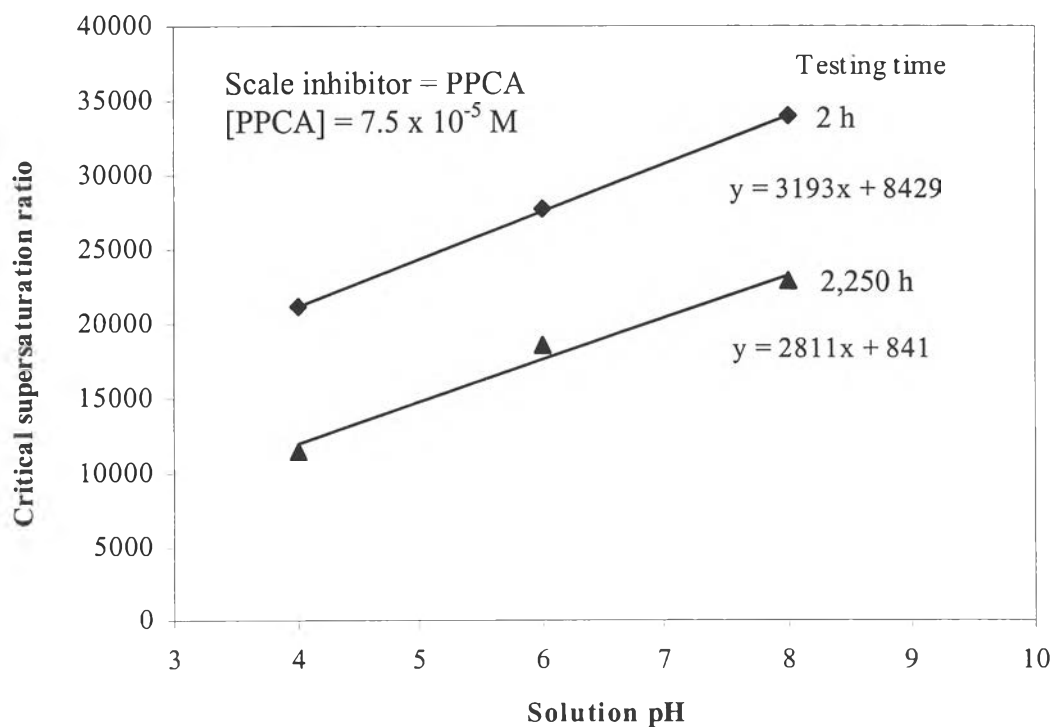
**Figure 4.26** The deprotonation curve of DTPMP and the resulting species composition as a function of solution pH.



**Figure 4.27** The effect of initial solution pH on the critical supersaturation ratio in the presence of ATMP.

**Figure 4.28** The effect of initial solution pH on the critical supersaturation ratio in the presence of DTPMP.
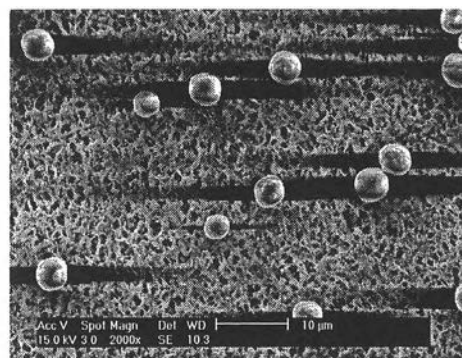


**Figure 4.29** The effect of initial solution pH on the critical supersaturation ratio in the presence of PPCA.

4.5.2    The Effect of Initial Solution pH on the Morphology of BaSO$_4$ Precipitates

Figure 4.30 shows the examples of the morphology of the BaSO$_4$ precipitates formed at different initial solution pHs. The results show that the initial solution pH strongly affected on the size and shape of the BaSO$_4$ precipitates. The higher the initial solution pH was used, the smaller size and more spherical shape of the BaSO$_4$ precipitate particles were observed. According to the fact that the scale inhibitors can be more deprotonated in a higher initial solution pH, consequently they contain more active sites to adsorb and block around the growing active sites of the forming BaSO$_4$ precipitates, resulting in the smaller and more spherical BaSO$_4$ particles in the same manner as increasing scale inhibition concentration.
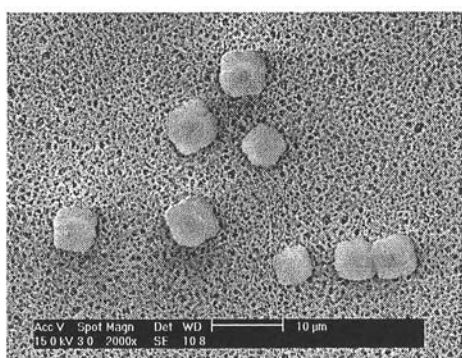


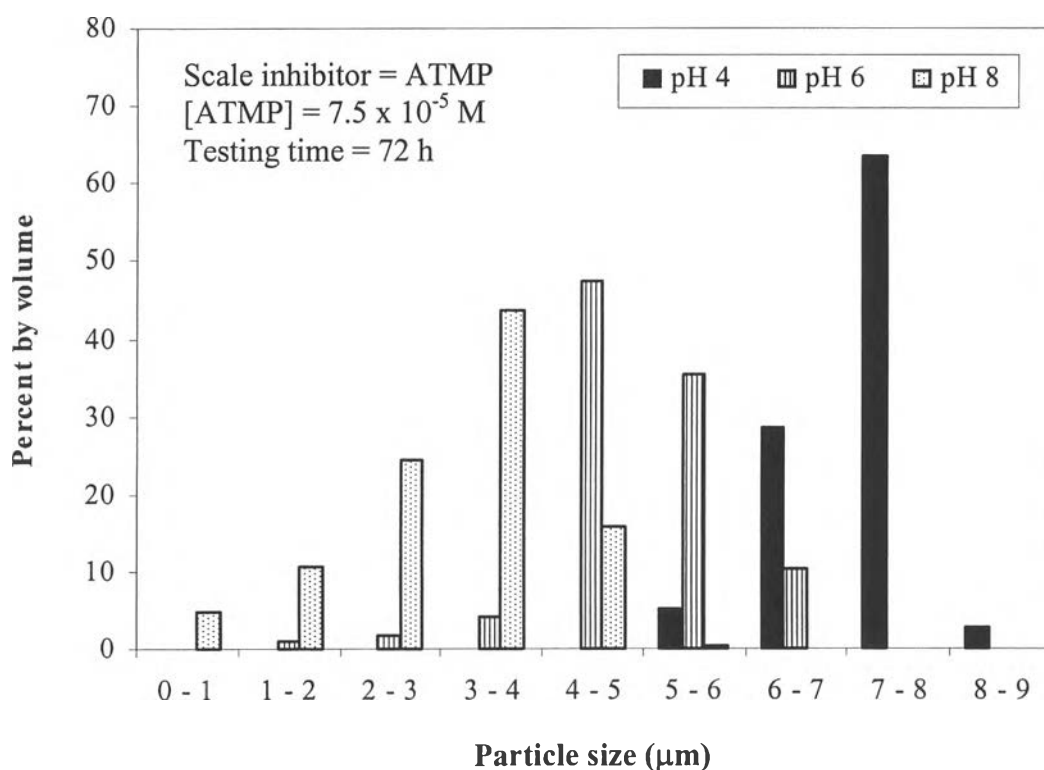(a) Initial solution pH 4 (2000X)          (b) Initial solution pH 6 (2000X)
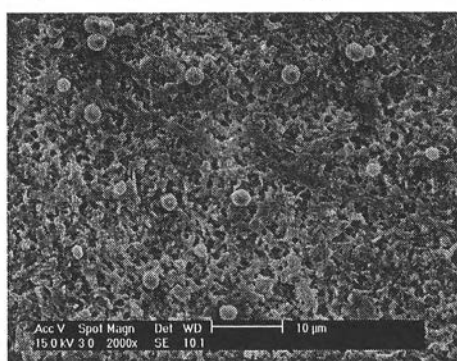


(c) Initial solution pH 8 (2000X)

**Figure 4.30** The morphological structures of the BaSO$_4$ precipitates for different initial solution pHs at testing time = 2 h in the presence of ATMP 7.5 x $10^{-5}$ M: (a) SR = 5,832, (b) SR = 5,832, and (c) SR = 7,402.
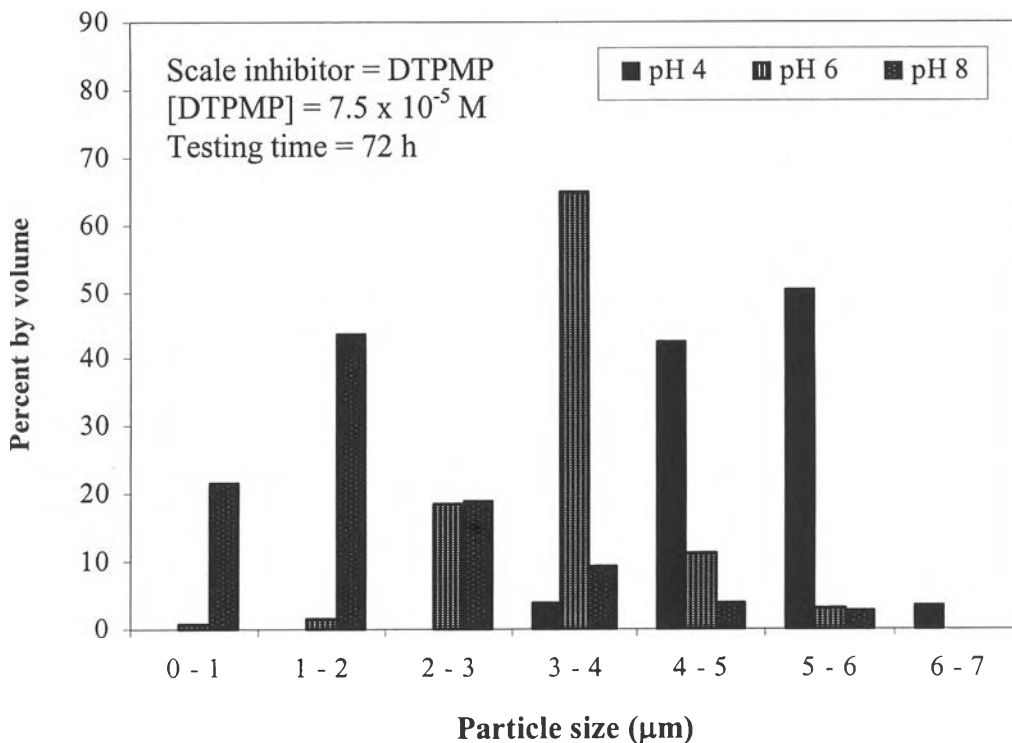
4.5.3    The Effect of Initial Solution pH on the Particle Size Distribution and
the Mean Diameter of BaSO₄ Precipitates

The effect of initial solution pH on the particle size distribution and the mean diameter of the BaSO₄ precipitates are shown in Figures 4.31 – 4.36, respectively. It is indicated that the broader the particle size distribution and the smaller the mean diameter of the BaSO₄ particles are resulted from increasing the initial solution pH. The capability for blocking the BaSO₄ particle growth substantially depends on the number of active sites of the scale inhibitors. When the initial solution pH increased, the more active sites are available for BaSO₄ inhibition as described before as in the case of increasing scale inhibitor concentration.



**Figure 4.31**  The effect of initial solution pH on the particle size distribution of the BaSO₄ precipitates in the presence of ATMP.
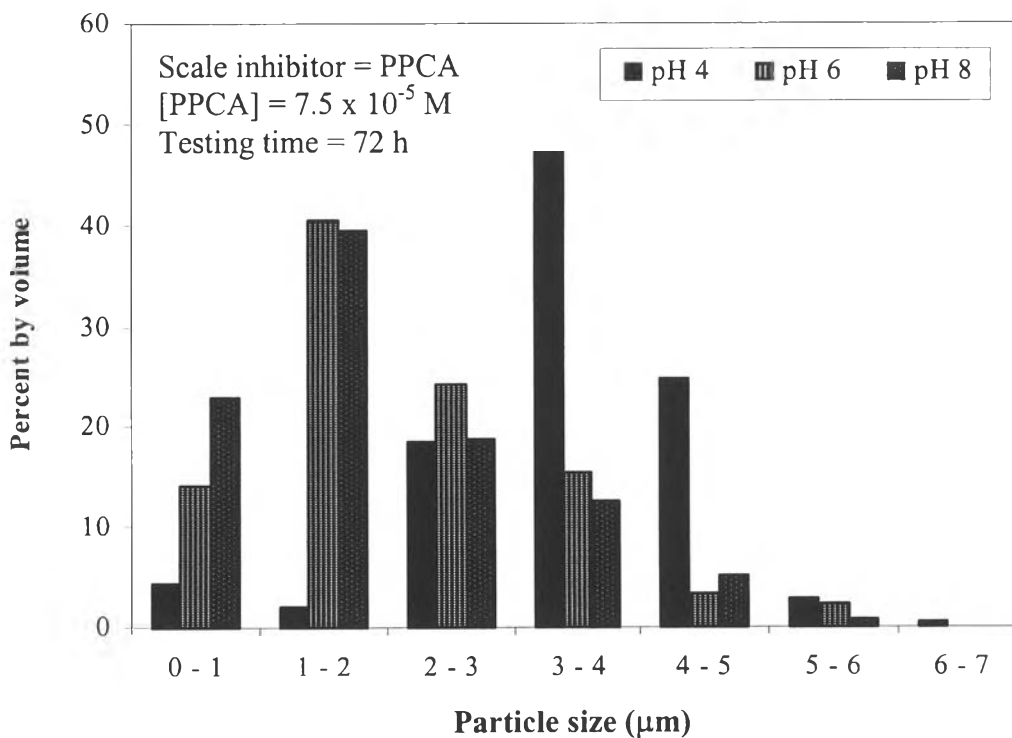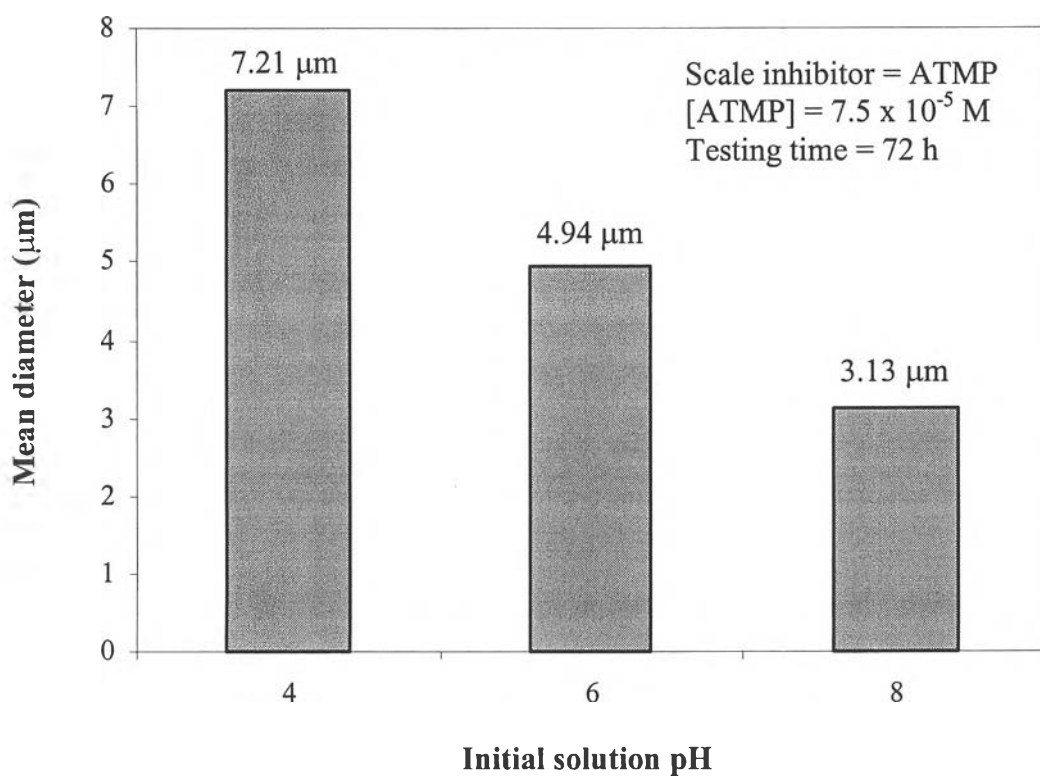
**Figure 4.32** The effect of initial solution pH on the particle size distribution of the BaSO₄ precipitates in the presence of DTPMP.
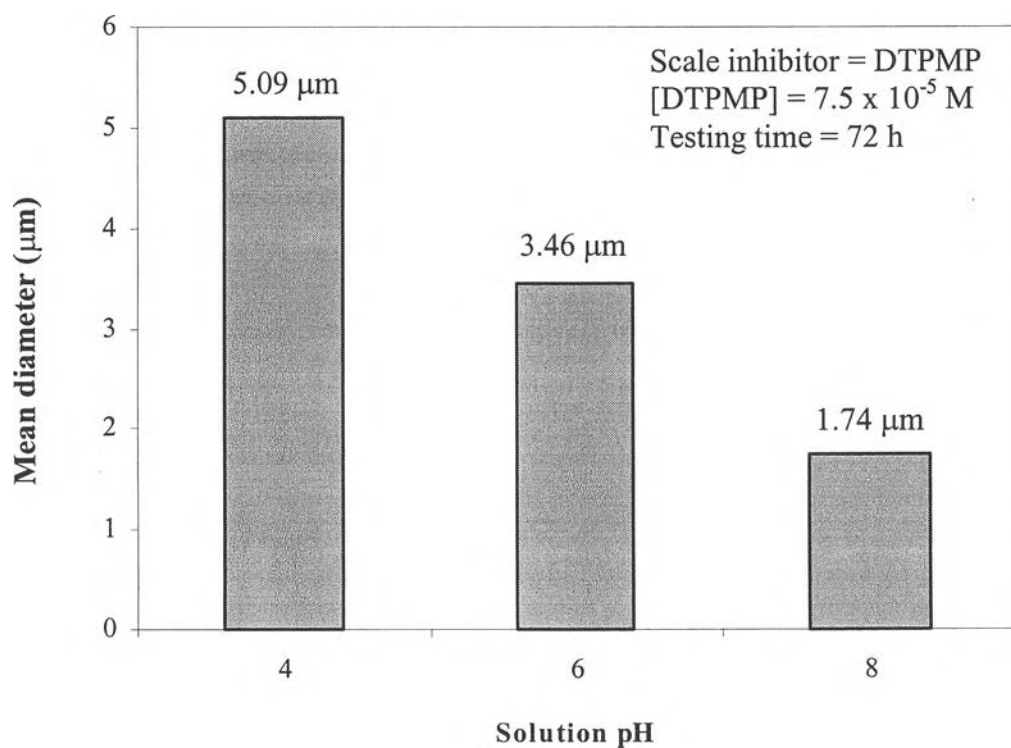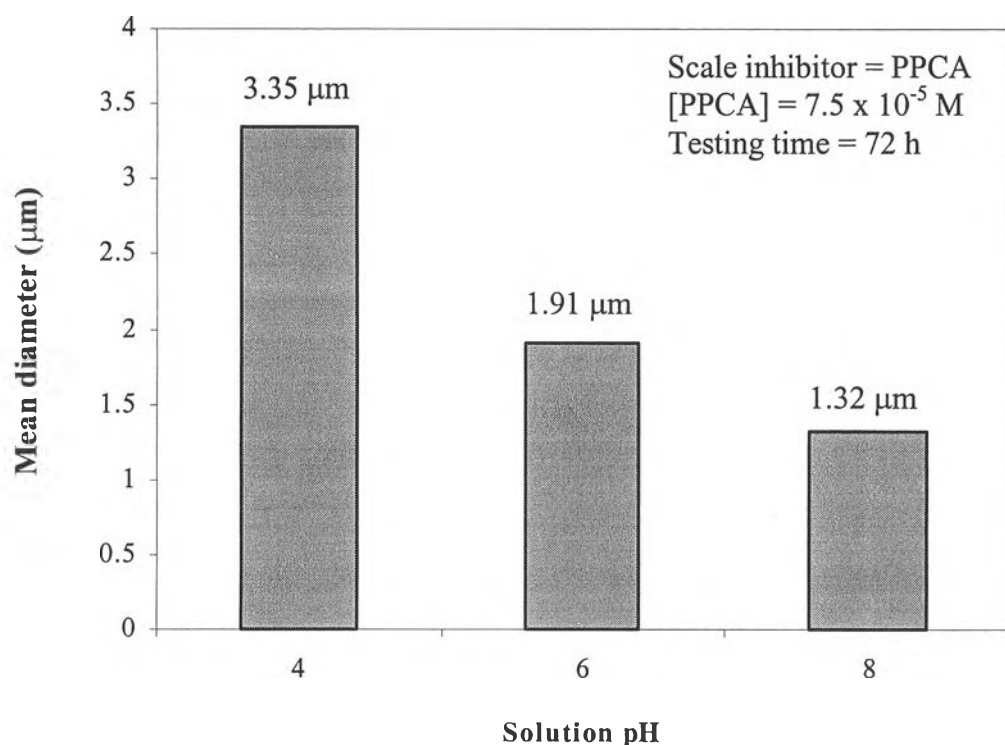


**Figure 4.33** The effect of initial solution pH on the particle size distribution of the BaSO₄ precipitates in the presence of PPCA.

**Figure 4.34**  The effect of initial solution pH on the mean diameter of the BaSO₄ precipitates in the presence of ATMP.



**Figure 4.35**  The effect of initial solution pH on the mean diameter of the BaSO₄ precipitates in the presence of DTPMP.

**Figure 4.36** The effect of initial solution pH on the mean diameter of the BaSO$_4$ precipitates in the presence of PPCA.

## 4.6 The Effect of Type of Scale Inhibitors

### 4.6.1 The Effect of Type of Scale Inhibitors on the Critical Supersaturation Ratio

The effect of type of scale inhibitors was studied with three commercial scale inhibitors including ATMP, DTPMP, and PPCA. Figure 4.37 shows the critical supersaturation ratios as a function of the testing times with those three scale inhibitors. It can be seen that the critical supersaturation ratio significantly decreased with increasing the testing time in case of ATMP, but in cases of DTPMP and PPCA, the gradual decreased in the critical supersaturation ratio with the testing times was observed.
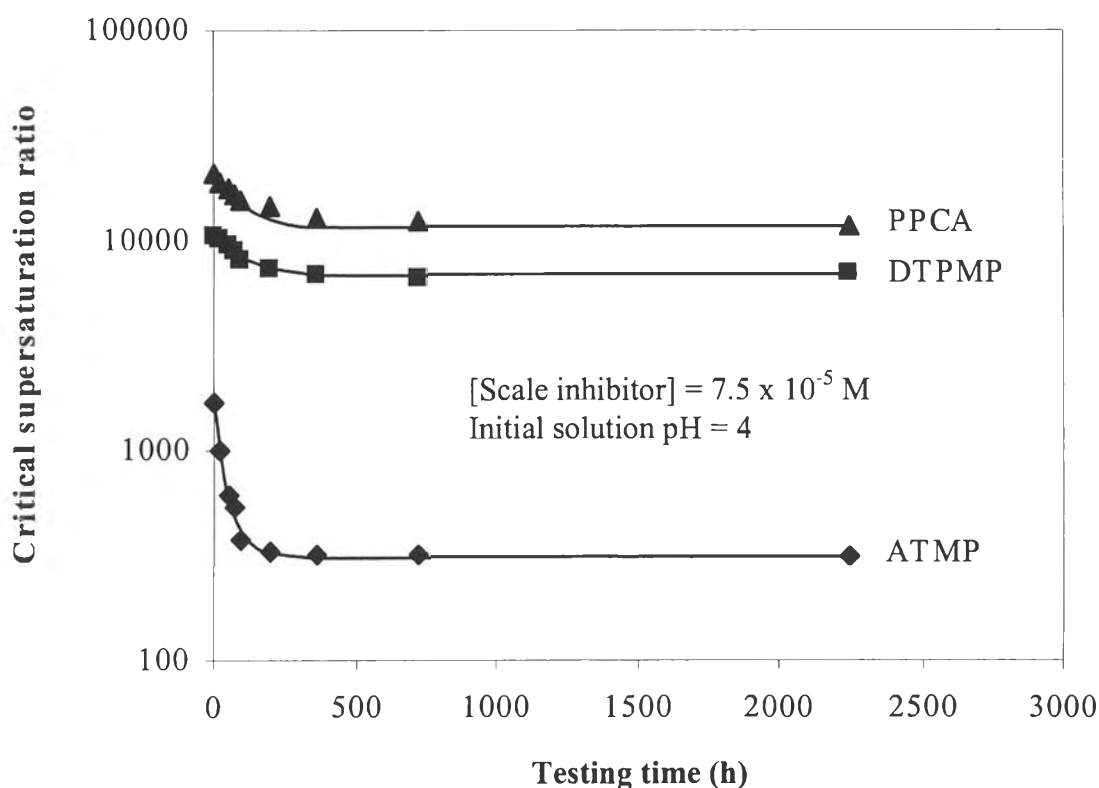
**Figure 4.37** The variation of the critical supersaturation ratios with the testing times for different types of scale inhibitors.

Furthermore, the results indicated that at any given scale inhibitor concentration or initial solution pH, PPCA is more effective for $BaSO_4$ precipitate inhibition than DTPMP and ATMP, respectively, as shown in Figures 4.38 and 4.39. It can be explained that PPCA contains twenty five ionizable protons per molecule whereas DTPMP and ATMP have only ten and six ionizable protons respectively, therefore PPCA which contains much more active sites can provide higher capability of inhibiting the $BaSO_4$ precipitation and larger no-precipitation zone than DTPMP and ATMP, respectively. The structures showing the ionizable protons of these scale inhibitors are shown in Figure 3.1. At the same conditions of pH and scale inhibitor concentration, PPCA tends to be more deprotonated than DTPMP and ATMP, respectively, due to the equilibrium acid constants as also indicated in Table 3.1. In addition, as shown in Figures 4.38 and 4.39, the correlation between the scale inhibitor concentration and the critical supersaturation ratio and between the initial solution pH

and the critical supersaturation ratio for all 3 types of scale inhibitors are also semi-logarithmically linear and linear, respectively, as mentioned earlier.
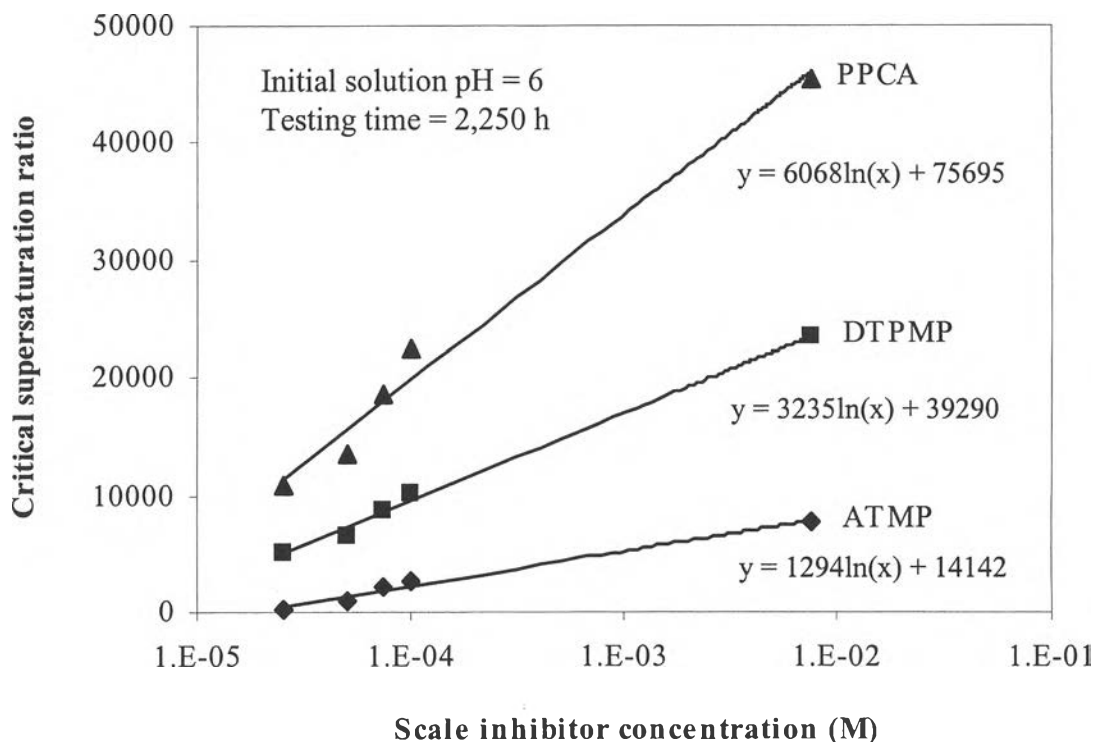


**Figure 4.38** The effect of scale inhibitor concentration on the critical supersaturation ratio for different types of scale inhibitors.

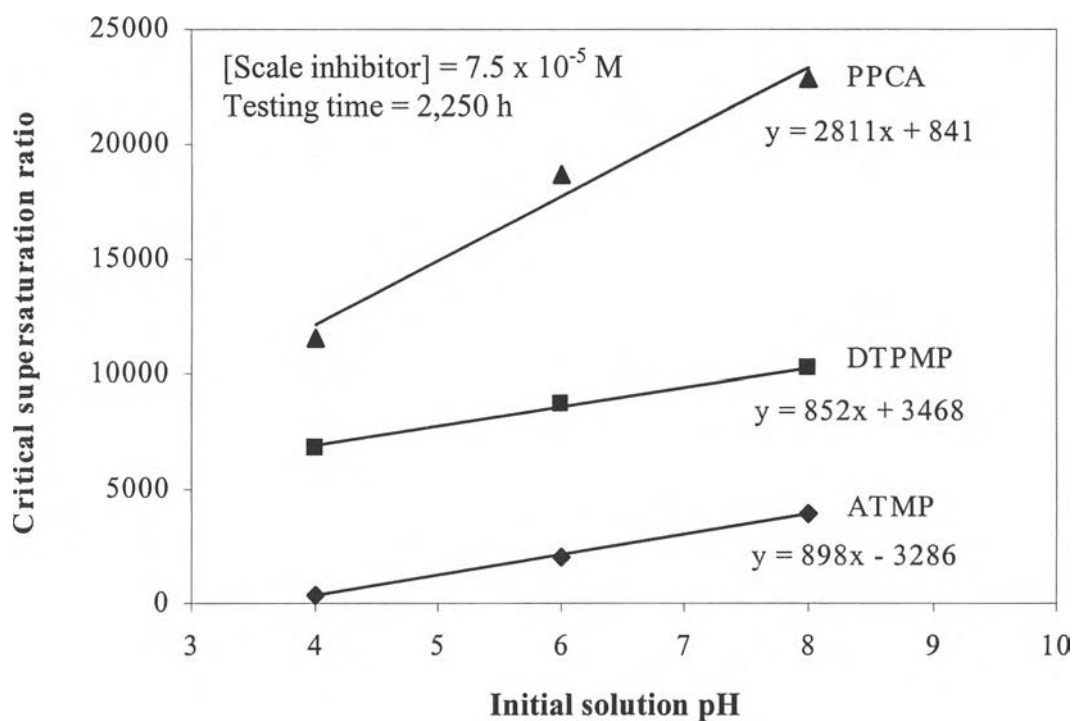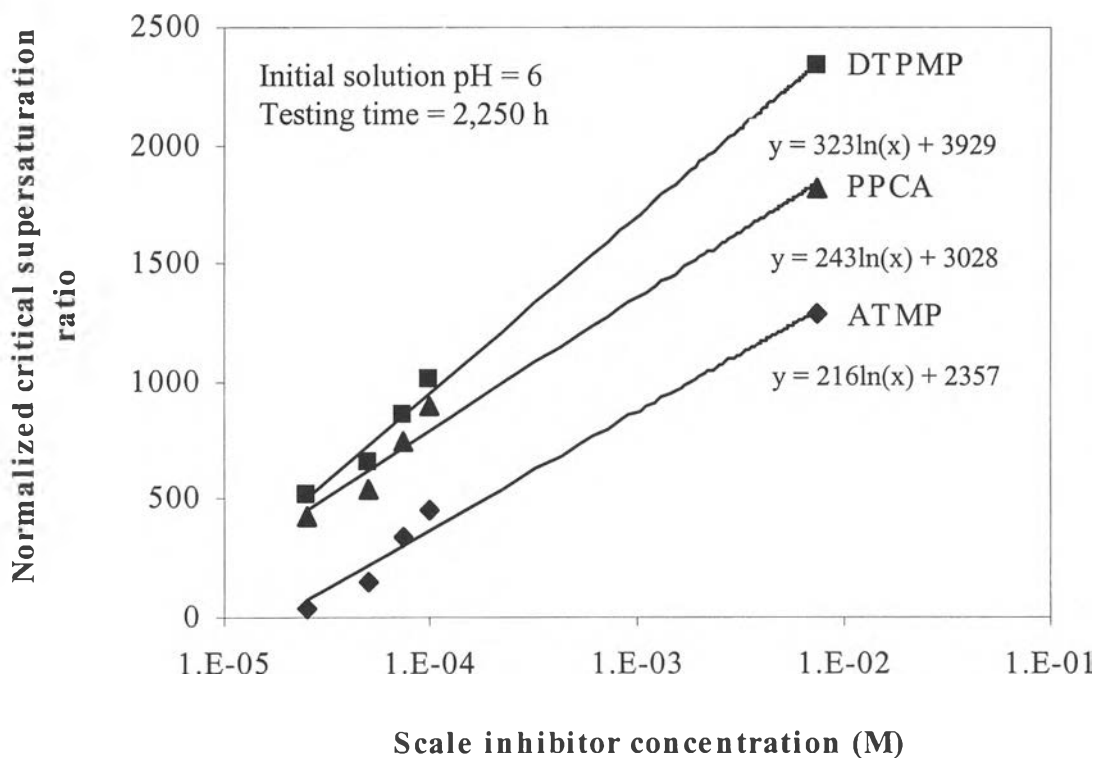### 4.6.2 The Effect of Type of Scale Inhibitors on the Normalized Critical Supersaturation Ratio

The critical supersaturation ratio data for all 3 types of the scale inhibitors were normalized by the number of ionizable protons contained in each scale inhibitor type to exclude the effect of different amounts of active sites. Figures 4.40 and 4.41 show the correlations between the scale inhibitor concentration and the normalized critical supersaturation ratio and between the initial solution pH and the normalized critical supersaturation ratio. The results are obvious that DTPMP provided higher efficiency for inhibiting $BaSO_4$ precipitation than PPCA and ATMP, respectively. The steric effect may play an important role on diminishing the inhibition efficiency of PPCA, which is a long chain polymeric molecule.

**Figure 4.39** The effect of initial solution pH on the critical supersaturation ratio for different types of scale inhibitors.



**Figure 4.40** The effect of scale inhibitor concentration on the normalized critical supersaturation ratio for different types of scale inhibitors.
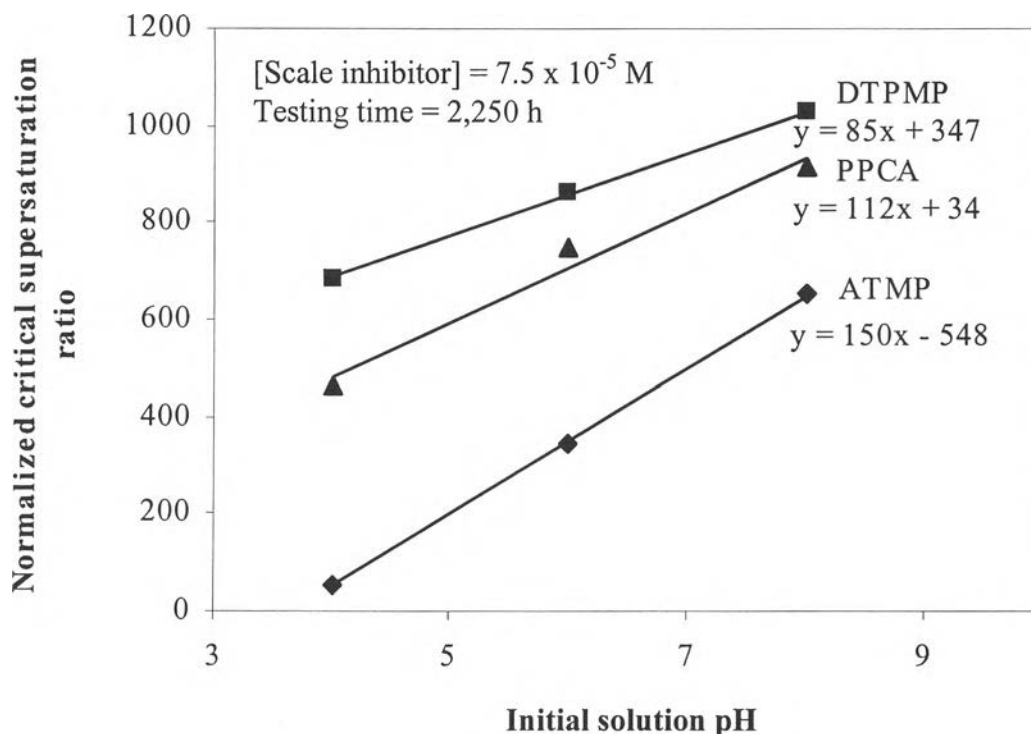
**Figure 4.41** The effect of initial solution pH on the normalized critical supersaturation ratio for different types of scale inhibitors.

### 4.6.3 The Effect of Type of Scale Inhibitors on the Morphology of BaSO₄ Precipitates

The exemplified morphologies of the $BaSO_4$ precipitates formed in the presence of ATMP, DTPMP, and PPCA are shown in Figure 4.42. The results show that the type of the scale inhibitors drastically affected on the particle size and the morphological structure of the $BaSO_4$ particles. The differences in the particle size and morphological structure could be observed. The particle size of the $BaSO_4$ precipitates in the presence of PPCA was much smaller than in the presence of DTPMP and ATMP, even at higher supersaturation ratios. Therefore, PPCA can preferably adsorb onto more active sites around the surface of $BaSO_4$ precipitates to DTPMP or ATMP due to the larger number of active sites from higher capability of deprotonation.

(a) In the presence of ATMP (2000X)        (b) In the presence of DTPMP (2000X)



(c) In the presence of PPCA (4000X)
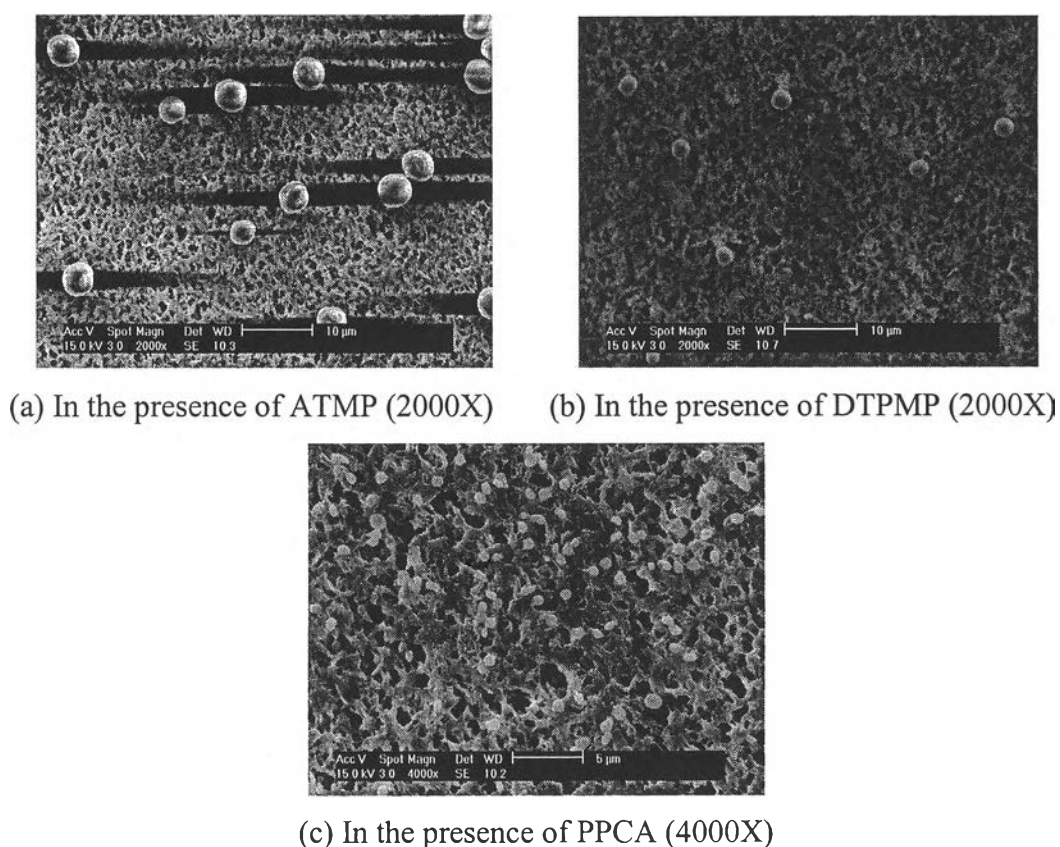
**Figure 4.42** The morphological structures of the BaSO$_4$ precipitates in the presence of different scale inhibitors at testing time = 2 h and scale inhibitor concentration = 7.5 x 10$^{-5}$ M: (a) SR = 5,832, (b) SR = 17,500, and (c) SR = 40,844.
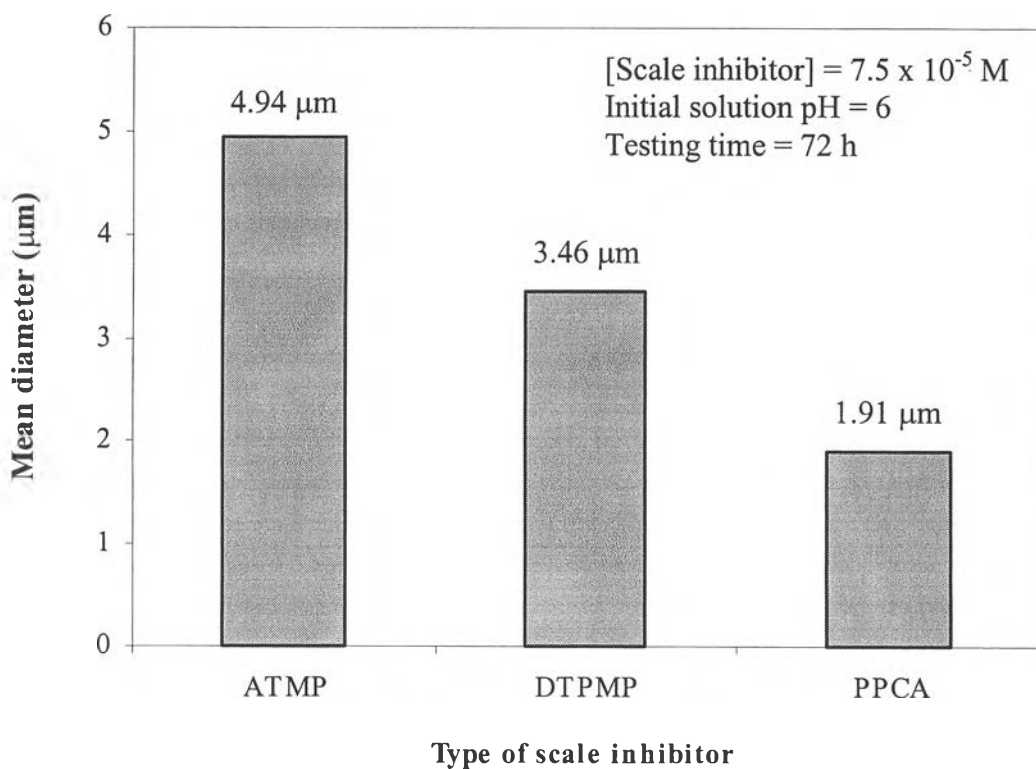
4.6.4   The Effect of Type of Scale Inhibitors on the Particle Size Distribution and the Mean Diameter of BaSO$_4$ Precipitates

The type of the scale inhibitors has significant effect on both the particle size distribution and the mean diameter of the BaSO$_4$ precipitates as shown in Figures 4.43 and 4.44. The results demonstrate that the BaSO$_4$ precipitates formed in the presence of PPCA had the broader particle size distribution and the smaller mean diameter than those in the presence of DTPMP and ATMP, respectively, because at any given condition, PPCA contains greater number of active sites in molecule than DTPMP and ATMP as previously explained.
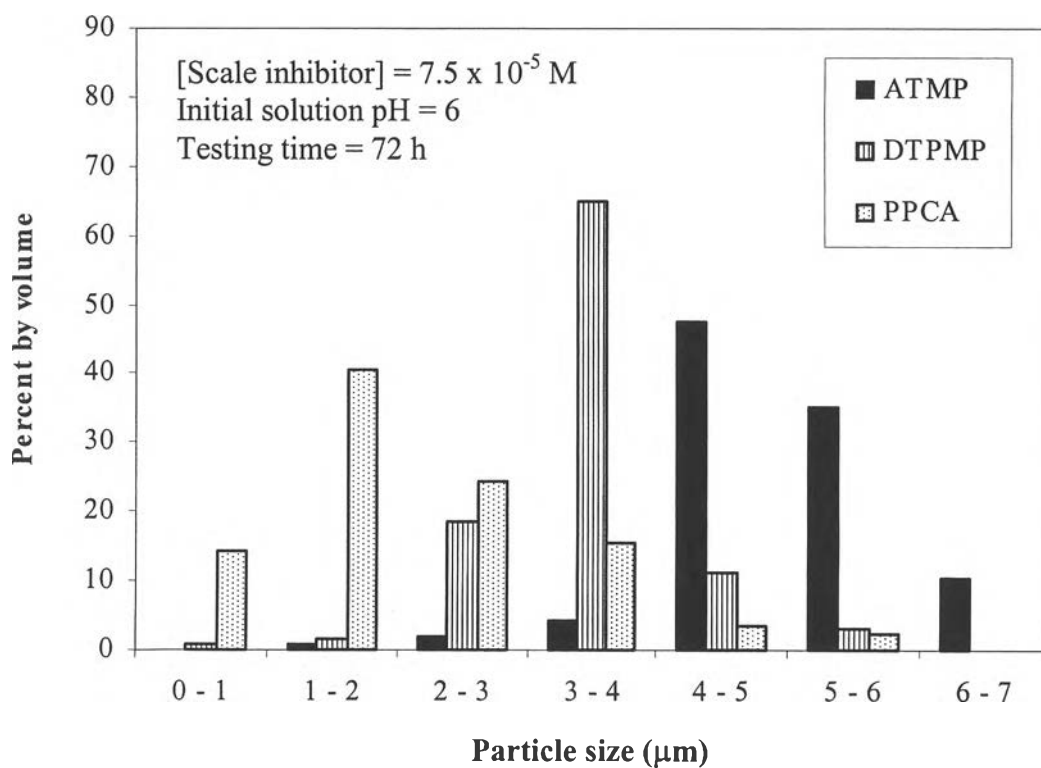
**Figure 4.43** The effect of type of scale inhibitors on the particle size distribution of the $BaSO_4$ precipitates.



**Figure 4.44** The effect of type of scale inhibitors on the mean diameter of the $BaSO_4$ precipitates.

## 4.7 Possible Interaction between Scale Inhibitors and Nucleated BaSO₄ Precipitates

During precipitation process, the barium cations ($Ba^{2+}$) and sulfate anions ($SO_4^{2-}$) contained in supersaturated solution react and finally form the $BaSO_4$ scale crystals. The nuclei of $BaSO_4$ are initially formed from the reaction between both ions. Afterwards, when the stable nuclei gradually growing in a supersaturated system become larger than the critical size, they start growing into crystals (Mullin, 1961). However, in the presence of the scale inhibitors, the crystallization tends to decrease because the scale inhibitors play an important role in lowering or completely preventing the formation and growth of $BaSO_4$ scales. Generally, there are two pathways to reduce or inhibit the scale formation and growth (Graham *et al.*, 1997):

1.  The scale inhibitors reversibly adsorb onto the growing sites of $BaSO_4$ nuclei. The adsorption is able to disrupt the thermodynamic stability of the nuclei. Therefore, some portions of the $BaSO_4$ nuclei are dissolved back into the original precipitating constituents and some portions adsorbed by the scale inhibitors are unable to further grow to become crystals.

2.  The scale inhibitors irreversibly adsorb and cling to the active growth sites of the growing $BaSO_4$ crystals. The adsorption can block the growth process of the crystals. Hence, the blockage of the crystals results in no longer growing.

Figure 4.45 shows the typical EDS elemental analysis of $BaSO_4$ precipitates synthesized in the experiments. The result indicates that the precipitates formed in the experimental supersaturation system were $BaSO_4$. It is obvious that the dominant mechanism in inhibiting the forming $BaSO_4$ precipitates is nucleation inhibition. The evidence is shown in the elemental compositions of the $BaSO_4$ precipitates because they contained only barium (Ba), sulfur (S), and oxygen (O) elements, without significant amount of other elements such as phosphorus (P) which is the elemental compositions of the scale inhibitors. During the nucleation inhibition, the scale inhibitors reversibly adsorb onto the $BaSO_4$ nuclei. Therefore, they can be easily removed from the active sites of the nuclei during washing of the $BaSO_4$ precipitates by the ultrapure deionized water prior to EDS analysis. If the crystal growth inhibition plays more important role than the nucleation inhibition, the elemental compositions

contained in the scale inhibitor molecules will be detected because the scale inhibitors irreversibly adsorb onto the growing $BaSO_4$ crystals and are subsequently difficult to be eliminated from the crystals by washing, e.g. the phosphorus (P) peak from the EDS analysis has to be apparently shown at X-ray energy of 2 keV. Thus, the inhibition of $BaSO_4$ scale precipitation by scale inhibitors is conclusively caused from reversible adsorption of active scale inhibitor molecules onto active growth sites of nucleated $BaSO_4$ scales.
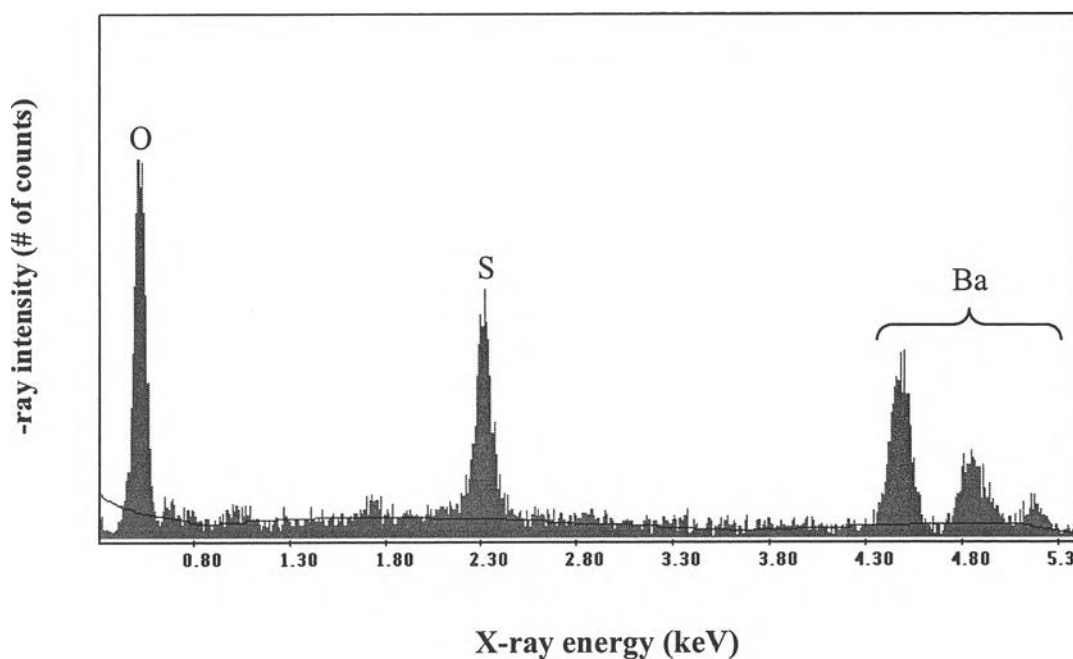


**Figure 4.45** The EDS analysis of the $BaSO_4$ precipitates.